NIVA

REPORT SNO 4198-2000

The international project on Ocean CO_2 sequestration

Ocean current measurements off Keahole Point, Hawaii, 5 August - 12 September, 1999

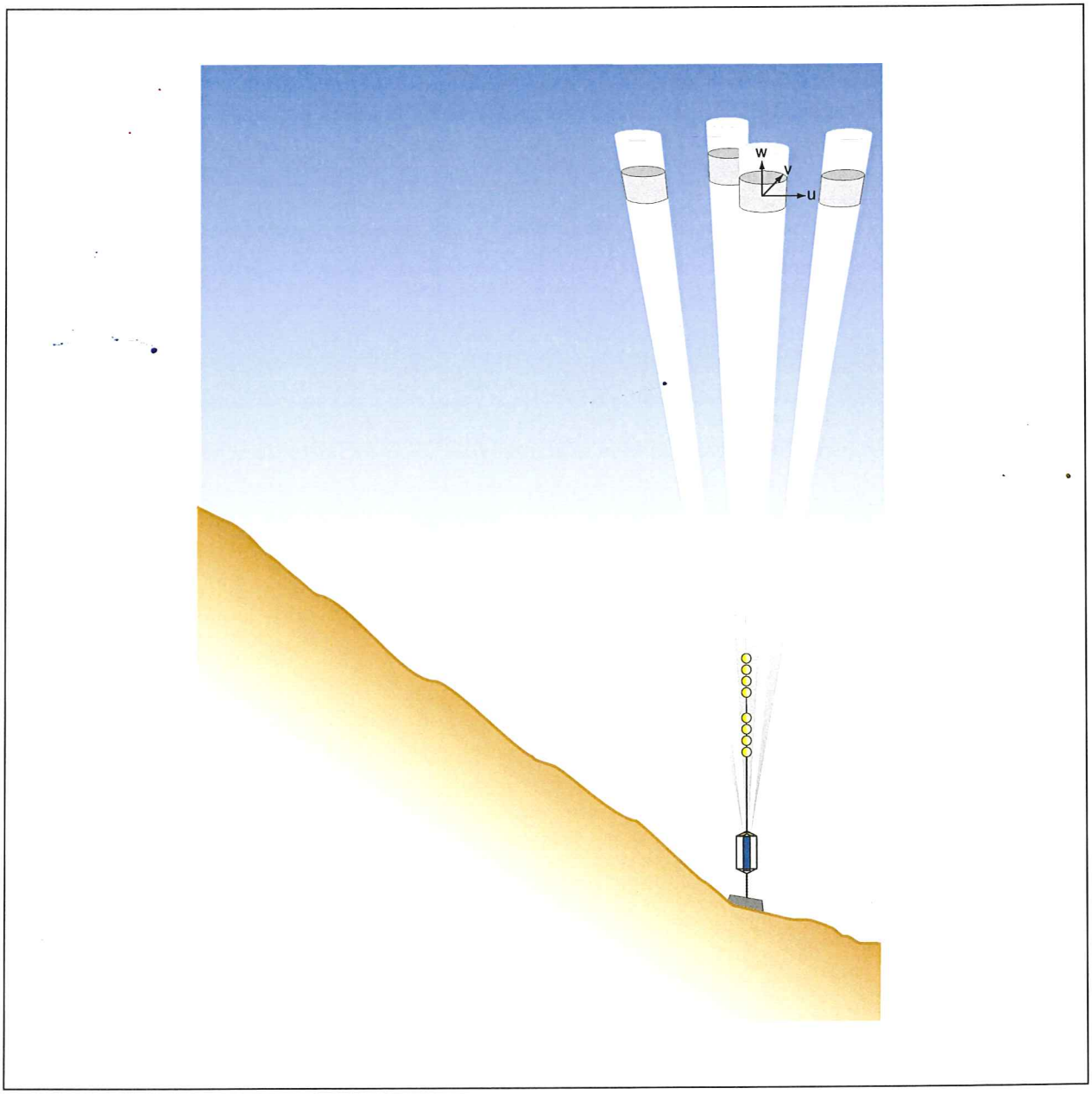

Norwegian Institute for Water Research

REPORT

Main Office
P.O. Box 173, Kjelsås
N-0411 Oslo
Norway
Phone (47) 22 18 51 00
Telefax (47) 22 18 52 00

Regional Office, Sørlandet
Televeien 3
N-4879 Grimstad
Norway
Phone (47) 37 29 50 55
Telefax (47) 37 04 45 13

Regional Office, Østlandet
Sandvikaveien 41
N-2312 Ottestad
Norway
Phone (47) 62 57 64 00
Telefax (47) 62 57 66 53

Regional Office, Vestlandet
Nordnesboder 5
N-5008 Bergen
Norway
Phone (47) 55 30 22 50
Telefax (47) 55 30 22 51

Akvaplan-NIVA A/S
N-9005 Tromsø
Norway
Phone (47) 77 68 52 80
Telefax (47) 77 68 05 09

Internet: www.niva.no

Title	Serial No.	Date
The international project on ocean CO_2 sequestration. **Ocean current measurements off Keahole Point, Hawaii, 5 August – 12 September, 1999.**	4198-2000	April 2000
	Report No. Sub-No. **O-97125**	Pages Price 104
Author(s) Arild Sundfjord Lars Golmen	Topic group Oceanography	Distribution
	Geographical area Hawaii/Pacific	Printed

Client(s)	Client ref.
The Norwegian Research Council, ABB, Statoil, Norske Shell, Norsk Hydro	NRC 120081/228

Abstract

The report presents data from an RDI ADCP and an Aanderaa RCM9 current meter deployed at ca. 800 m depth from August 5 – September 12, 1999, off Keahole Point on the Big Island of Hawaii. The measurements were part of the international project on ocean CO_2 sequestration. The ADCP measured 3D currents from 763 m to 259 m depth in 85 separate cells, each of 6 m thickness. The recording interval was 40 minutes, while the RCM9 at 10 m above the bottom sampled at 10 min. intervals. Average speed measured by the ADCP increased upwards from ca. 4 cm/s near bottom to 5.5 cm/s at 500 m depth and 10.5 cm/s in the shallowest cell. Corresponding maximum currents were ca. 15, 17 and 45 cm/s. The RCM9 showed average and maximum speeds of 4 and 15 cm/s respectively. The main flow was along the NW-SE axis, with SE flow dominating the deeper layers and NW the shallower ones with a shear zone at around 500 m depth. Tides of diurnal and semi-diurnal period dominated the energy field, while shorter periods had peaks around 1 and 2 hours, corresponding to resonating, bottom modified internal waves.

4 keywords, Norwegian	4 keywords, English
1. Havlagring av CO_2	1. CO_2 ocean sequestration
2. CO_2 eksperiment	2. CO_2 experiment
3. ADCP	3. ADCP
4. Hawaii	4. Hawaii

Project manager	Research manager	Head of research department
Lars G. Golmen	Jan Magnusson	Bjorn Braaten

ISBN 82-577-3817-4

O-97125

The international project on Ocean CO_2 sequestration

Ocean current measurements off Keahole Point, Hawaii, 5 August – 12 September, 1999

Preface

The measurements with the RDI ADCP and the Aanderaa RCM-9 off the Kona coast in Hawaii in 1999 were successfully completed, thanks to thorough preparatory work and deployment assistance from the crew of the R/V ‘Ka’imikai-O-Kanaloa’ (KOK) and on-shore assistance from PICHTR and the U of Hawaii.

Chief scientist for the August cruise with R/V 'KOK' was Dr Eric Adams from MIT. Dr. Rick Coffin from the Naval Reseach Laboratory was the contract responsible for the vessel. Arild Sundfjord and Lars Golmen from NIVA, Norway, in co-operation with the crew of the 'KOK', carried out the deployments. Professor Malahoff, University of Hawaii, kindly gave us the opportunity to use part of their cruise time in September with the 'KOK' to retrieve the instruments.

ABB Corporate Research Ltd., Switzerland, provided support to the activities through financing of the ADCP instrument. The Norwegian Research Council, Statoil, Norske Shell and Norsk Hydro supported the work undertaken by Norway, including the preparation of this report. Ship time was provided by the NRL through a grant from the US/DOE.

Thanks are particularly due to Steve Masutani and Gerard Nihous in assisting with all the preparations for the measurements. We are also indebted to the shore personnel of the U of Hawaii Shipboard Technical Assistance Group (STAG) and not least to the crew of the R/V 'KOK'.

Thanks also to Einar Nygaard at Statoil who helped out with the tidal analyses.

Bergen, April 2000

Arild Sundfjord *Lars G. Golmen*

Contents

Summary

As part of the International Project on Ocean CO_2 Sequestration some oceanographic studies were carried out at a proposed experiment site off Keahole Point, Hawaii during a research cruise with the R/V Kaimikai-O-Kanaloa, 03 – 08 August, 1999. Hydrography and pH were measured and samples for analysis of carbon chemistry, bacteria and sediments were collected. These results have been reported elsewhere. Additionally, two deep moorings with current meters were deployed on 05 August. One mooring was furnished by NIVA, Norway, and deployed at 790 m bottom depth. It contained one single-point Doppler current meter (Aanderaa RCM9) 10 m above the bottom, and one upward facing RDI Long Ranger Acoustic Doppler Current Profiler (ADCP) mounted 3 m above this. Results from these two instruments are the focus of this report.

A second mooring, supplied by RITE, Japan, consisted of three point measuring acoustic current meters (ACMs) at 410, 630 and 855 m depth. These were programmed for high frequency sampling, and the results are published in a separate report (Maeda et al. 2000). Both moorings were retrieved on 12 September, 1999, and the subsequent data analysis showed that the instruments had been operating successfully throughout the five week deployment with data return as intended and satisfactory data quality. It can initially be stated that a comparison between measurements from the different instruments on the two moorings showed very good correlation and similar statistics.

By applying the Doppler shift, the Long Ranger ADCP measures the direction and 3D velocity of the water current in many depth cells in the water coloumn above the instrument. It sampled at 9.6 sec intervals, and was programmed with a 40 minute recording interval. By making measurements in 85 cells of 6 m thickness each, the depth range from 259 m to 763 m (27 m above the bottom) was covered by current measurements. The RCM9 sampled horizontal current and in addition sea temperature, salinity and turbidity at 10 minute intervals.

The current speed generally increased from the bottom and upwards. Average speeds ranged from around 4 cm/s in the lower ADCP cells to 5.5 cm/s at 500 m and 10.5 cm/s in the uppermost cell. Corresponding maximum currents were ca. 15, 17 and 45 cm/s. There seemed to be a distinct shear zone at around 500 m depth, with different regimes for both speed and direction below and above this depth. Below, the current was quite homogeneous in terms of average and maximum speed and variability was moderate throughout the period. In the upper part, there were distinct periods of 1-2 days duration with stronger fluctuations.

Above 500 m depth, the current was almost exclusively towards the NW for the first half of the measurement period. Later, the current was more influenced by the tide, changing between NW and SE directions. The deeper parts had water moving mostly to the SE, but also with frequent tidal bursts to the NW. SE flow dominated the deeper layers and NW the shallower ones.

The RCM9 at 10 m above the bottom gave average and maximum speeds of 4 and 15 cm/s respectively. SE direction dominated, with intermittent periods with NW flow. The residual current at this depth was directed at 117^o, i.e. towards E-SE.

Significant instantaneous vertical current shear was found at all depths, with values in the order of 0.01-0.02 /s on several occasions. In particular, strong vertical current shear was observed in the upper parts of the measurement range. Tidal harmonic constants have been calculated for some selected depths, to give more insight into the tidal influence at the location. The diurnal and semi-diurnal components were most prominent. Spectral analyses of current speed time series for the RCM9 showed peaks around 1 and 2 hours, probably corresponding to resonating internal waves modified according to the local bottom slope of about 25^o.

Calculations on the duration of different current "events" were made, by finding the duration of average and longest period with the current staying un-interruptedly above or below a certain value and additionally for how long the current was stationary in direction. On the average, currents near the bottom (RCM9) remained constantly below 2 cm/s for ca. 20 minutes only and below 6 cm/s for 1.5 hours, while the longest measured periods were ca. 50 minutes and 12 hours, respectively. Due to rapid directional variation between 30^o sectors at this depth the current remained inside one such sector for about 15 minutes only, before swinging into the neighbouring sector. Further up, the directional variation was less, with corresponding duration of about 45 minutes to an hour.

The ADCP also measured vertical velocities. Vertical motions prevailed throughout the water coloumn, and the time integrated flux was downward at all depths. Strong indications of vertically migrating zooplankton have been found at depths between 260 and 400 m. At nightfall, there is vigorous upward migration and at dawn these scatterers move back down. These observations are backed by corresponding increases and decreases in the strength of the ADCP return signal in the depth cells in question, i.e. an increased return signal in the upper part (above 375 m depth) during night and a reduced signal at night below this.

The acquired data should be useful for the groups involved with the technical experiment design, numerical modellers, and for the planning of monitoring operations when the CO_2 injection takes place. Many aspects and parameters of this comprehensive data material remain to be analysed, according to specific user demand and purposes.

1. Introduction

1.1 Background and purpose

In 1997 an agreement on performing a CO_2 ocean sequestration experiment at a selected ocean site was reached among the countries Japan, USA and Norway. Later, Canada, Australia and several industrial companies have joined the experiment. Keahole Pt. and the research facility NELHA on the W side of the Big Island of Hawaii (**Figure 1**) is one candidate site for the experiment. The project calls for actions to collect data on the ambient environment, prior to the injection experiment itself which is planned to take place in the year 2001.

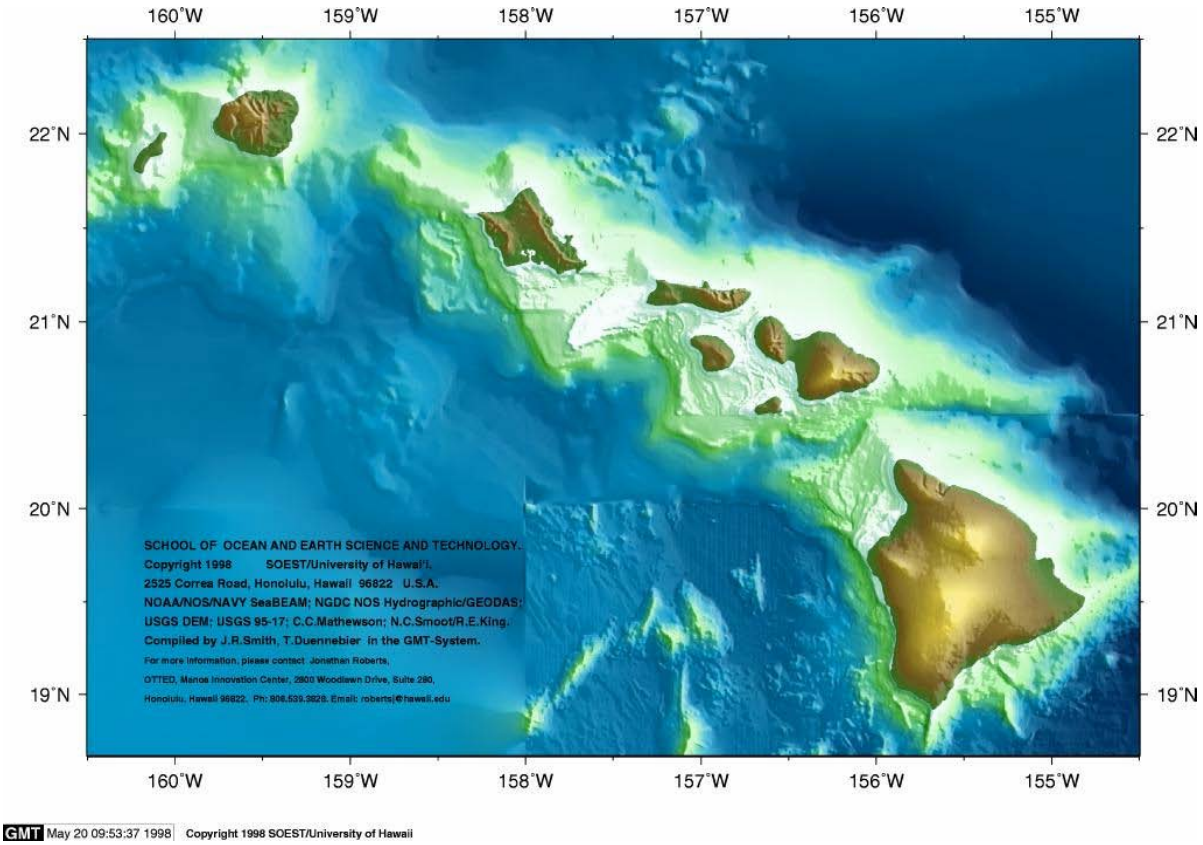

Figure 1. The Hawaii Islands, with the Big Island of Hawaii to the far right. Keahole Pt. is on the westernmost point on the Big Island.

Data on local hydrography, currents and ocean chemistry are needed for the detailed design of the experiment. It will also be important to have such data available in real-time during the conduction of the experiment, and planning for this continues separately. In 1998 it was agreed to have a cruise near or at the site, to gather supplementary information on oceanography, bottom topography, sea water chemistry and some biology. Planning for such a cruise went on in 1998 and into 1999, and thanks to additional funding and in-kind contributions from the Naval Research Laboratory (NRL) 8-10 days of cruise time with the research vessel 'Ka'imikai-O-Kanaloa' (KOK) from the University of Hawaii was obtained for the summer of 1999. This also included ship time to pick up moorings after about one month.

R/V 'KOK' left it's home port in Snug Harbor, Honolulu on 03 August, 1999. After completing some CTD stations en route to the Big Island, the investigation off Keahole Pt. began on 04 August, with

CTDs and sea water sampling. Day # 3, 05 August, was devoted to the deployment of two current meter moorings, at around 800 m bottom depth. NIVA, Norway, deployed a rig with one RDI Long Ranger ADCP (Acoustic Doppler Current Profiler) and one Aanderaa RCM9 (singular point acoustic Doppler current meter) just above the bottom. The instruments were provided by NIVA/ABB and rig harness and buoyancy provided by the UH' STAG group in Honolulu. RITE, Japan, deployed a mooring with three FSI 3D-ACMs (Three Dimensional Acoustic Current Meter) and pH probes at 20, 230 and 440 meters above the sea bottom. All instruments were recovered on a cruise with the KOK on 12 September, 1999.

The main purpose of this report is to present results from the instruments of the "Norwegian mooring". The CTD data were summarised by NIVA in a previous report (Sundfjord et al. 1999), and results from the Japanese mooring were reported by CRIEPI (Maeda et al. 2000).

The moorings were positioned as shown in **Figure 2** below. The bottom depth at the two rig locations was ~874 m (RITE) and ~790 m (NIVA).

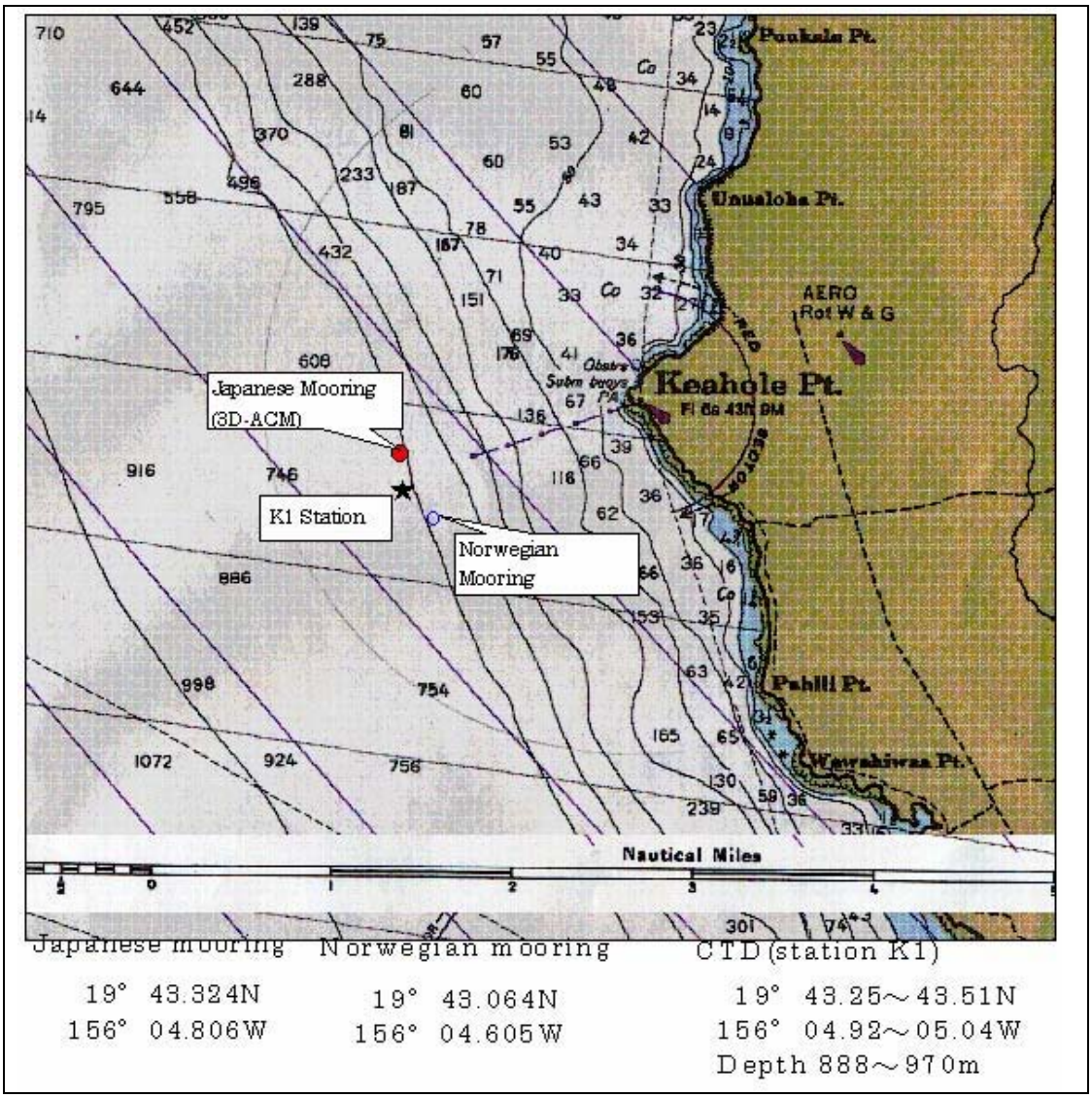

Figure 2. Chart showing the positions of the two current measurement rigs outside Keahole Point. Sampling station K1 from the R/V 'KOK' cruise, 3-8 August, is also shown. Depths are in fathoms, 1 fathom = 1.83 m.

2. Instrument Characteristics and Rig Design

2.1 RDI Long Ranger ADCP

The RDI Long Ranger Acoustic Doppler Current Profiler uses the so-called Doppler principle to measure velocities in the water. Sound signals with a particular frequency are sent from the instrument's hydrophones. Part of the signal is reflected by particles, bubbles etc. in the water above the instrument. If the particles are in motion relative to the source of the sound signals, the sound waves reaching them will have a slightly different relative velocity (and thus also frequency) than the original signal does. The particles themselves act as moving acoustic emitters when the signal is reflected back to the instrument, and the return signal will thus have twice the shift in frequency (Gordon, 1996). It is important to bear in mind that it's actually the particle motion and not the water current itself that is measured. Although these are virtually identical most of the time, it's not always the case. In areas with pipe outlets with negative buoyancy or extensive biological activity, the difference can be substantial and must be taken into account.

The Doppler frequency shift, Fd, can be calculated from Fd= 2Fs(V/C), where Fs is the frequency of the original sound wave, V is the speed of the particle relative to the hydrophone, and C is the speed of sound in the water. The speed V of the particles can thus be found as V=(C/2)(Fd/Fs). Note that this represents movement in the same direction as the original sound signal. If the particles are moving in a direction with an angle A relative to the sound waves, the above equation must be modified to V=(C/2cosA)(Fd/Fs). To determine current velocity in more than one direction, several hydrophones must be utilised by the same instrument. By sending signals in three directions, the three dimensional speed at a particular distance from the instrument may be found. Since this implies combining vector values from three different locations, the assumption that the current is homogeneous in a given horizontal layer must be made.

After sending out a ping (a single sound signal), the ADCP recives a continuous flow of echoes from particles at different distances. The further away from the sender the reflecting particle is, the longer it takes for the echo to reach the instrument. By separating the spectre of return signals into given time intervals, the current in different depth cells can be found. Due to the geometry of the system, the best representation of the current will be at the centre of each cell. There is also a certain degree of overlap between adjacent cells. The results can then be presented as a sort of point measurement with a certain amount of spreading, or mathematical weighting can be applied to even out the different contributions and give a value that is more representative for the entire cell. No matter how this is done, the separation into depth cells implies that the smaller scale vertical structure of the current can be lost.

There are different ways of recording and refining ADCP data. To minimize measurement uncertainty and conserve data storage capacity it is usual to record averaged data directly in the instrument itself. Depending on the type of current feature one wants to observe and how long the measurement period is, intervals without measurements can also be included in the measurement program, to save battery power and data handling capacity.

The RDI Long Ranger uses four transducers. This introduces a higher degree of accuracy than using only the three beams strictly necessary for resolving three dimensional currents. Vertical velocities in particular are measured with better resolution. In addition, the four beam system allows for better analysis of the relationship between instrument signal strength, ambient noise levels and the return signal received by the instrument – indicators of measurement accuracy. Further instrument specifications as supplied by RD Instruments are shown in Appendix D.

2.2 Aanderaa RCM9

This instrument also applies the Doppler principle to measure particle motion. The RCM9 emits sound waves in two orthogonal beams in a horizontal plane, and thus uses the return signals (within a given time interval) to obtain two dimensional current magnitude and direction at the instrument depth. To get as exact values as possible for the local speed of sound, the RCM9 is also equipped with sensors for temperature, conductivity and pressure. Furthermore, a turbidity sensor is integrated in the instrument. This allows for more accurate measurements of particle concentration. Data on each of the different sensors is included in Appendix D.

2.3 Deployment information

The RDI ADCP was programmed to measure with a pinging rate of 9.6 seconds. To achieve a maximum standard deviation (as given by the manufacturer's specifications) of 1.0 cm/s, 250 single measurements were averaged into ensembles. The time between these ensembles was thus 40 minutes. It would have been possible to set a higher pinging rate and shorter interval between ensembles, but for the batteries to last throughout the entire deployment period of 40 days a relatively long ensemble interval was unavoidable.

The RDI ADCP is capable of measuring the current in up to 128 cells of 4 to 32 meter vertical extent, with a maximum measuring range of about 600 m. Battery consumption depends on the number of individual acoustic pings the instrument sends out. The smaller the cells, the more pings are necessary per ensemble in order to reach an acceptable standard deviation level. The time interval between ensembles also influences battery use. By choosing 6 m cell height and a 40 minute ensemble interval, it was possible to cover a maximum total vertical range and still not risk to run out of energy before recovery of the mooring. Current was measured in a total of 85 depth cells. The water column from 763 m to 259 m depth was thus covered in the measurement series. (It is considered unlikely that the injected CO_2 will rise to depths beyond this range.)

For an ADCP to be able to differentiate between return signals from different cells, the first cell is always located at a minimum distance away from the instrument's transducers. In the Hawaii deployment, this so-called blanking distance of the RDI was about 14 m (distance from instrument to centre of first cell, the exact value depends on water characteristics (sound of speed)).

The Aanderaa RCM9 was programmed to record measurements with a 10 minute interval. The number of measurements made within the recording interval is set automatically by the instrument itself.

Deployment information for the two current meters is summarized in **Table 1**.

Table 1. Information on the instruments deployed near Keahole Point, August – September, 1999.

	RDI Long Ranger ADCP	**Aanderaa Instruments RCM9**
Instrument number	SN 0923	25
Instrument depth	777 m	780 m
Measurement depth	259 - 763 m	780 m
Position, North	19 43.064 N	19 43.064 N
Position, South	156 04.605 W	156 04.605 W
Deployment time *	20:30 August 5, 1999	20:30 August 5, 1999
Moooring retrieval *	23:30 Sept. 12, 1999	23:30 Sept. 12, 1999
Logging interval	40 minutes	10 minutes

* Time given in UTC (GMT)

2.4 Mooring design

The instruments were mounted in a mooring as shown in **Figure 3** below. A bottom weight of 500 kg was attached to a 5 m steel chain holding a MORS Acoustic Release. This was in turn connected to the Aanderaa RCM9 with a 2 m chain. Another 2 m above this, the RDI ADCP was attached. Starting at around 15 m above the RDI was a line of 12 Benthos subsurface buoys with a small pickup buoy in the upper end.

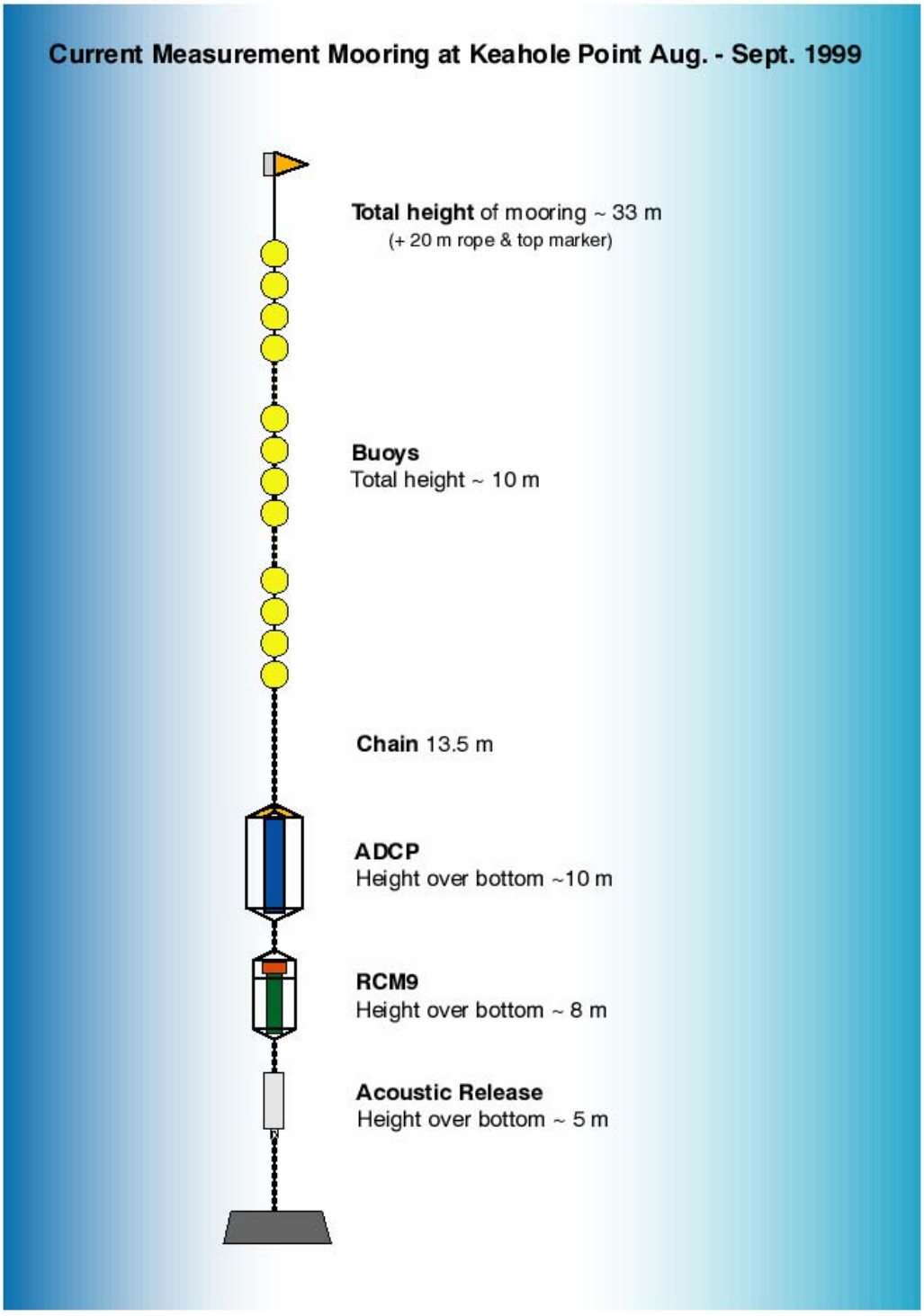

Figure 3. Layout of NIVAs current measurement mooring.

3. Data presentation

3.1 RDI ADCP

3.1.1 Horizontal velocities

The first valid data from the RDI ADCP were collected at 00:20 August 6 and the last good recording before retrieval was made at 14:20 September 12, giving a total of 1354 current ensembles for this instrument. **Figure 4** gives an introductory view of these current measurements. The graph shows current magnitude (contoured field, using a triangulation method) for all 85 depth cells and all ensembles. A few features are evident; the strongest current is usually found higher up in the water column. Also, strong currents are normally not limited to only a few cells, but extend over many cells.

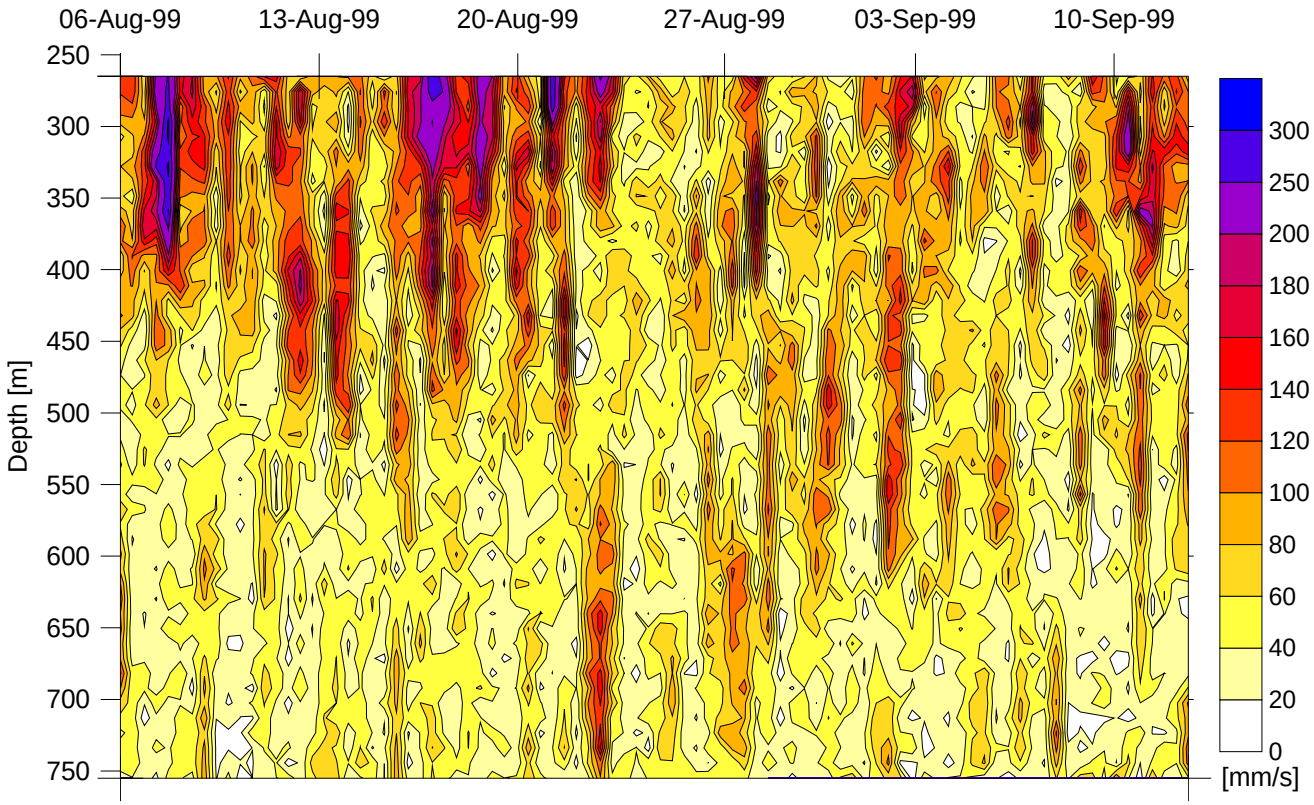

Figure 4. Contours of current magnitude for all cells and ensembles from the ADCP measurements.

Some statistical values are shown for every 50 meters in **Table 2**. The residual current calculated represents the overall vector average; a sort of equivalent, unidirectional current for the whole measurement period. The stability factor (range 0 – 1) is a measure of how much the direction varies – the higher the number, the more uniform is the current in terms of direction. This coefficient is calculated by dividing the residual current magnitude by the average absolute current magnitude.

Table 2. Selected current statistics at 50 m intervals, based on the whole measurement period. Current magnitudes are given in mm/s, direction in degrees. Stability is non-dimensional.

Cell #	Depth [m]	Average Current Magnitude	Maximum Current Magnitude	Standard Deviation	Residual Current Magnitude	Residual Current Direction	Stability Factor
85	259	104.3	446.0	68.0	59.4	326.4	0.57
78	300	97.6	397.0	62.7	52.4	324.0	0.54
70	350	86.6	322.0	49.9	46.4	321.5	0.54
61	400	76.0	259.0	42.1	36.0	322.6	0.49
53	450	63.0	207.0	36.9	22.1	324.0	0.35
45	500	55.6	171.0	30.8	1.0	21.3	0.02
36	550	52.1	175.0	30.1	16.5	145.2	0.32
28	600	51.9	186.0	29.6	23.7	144.8	0.45
20	650	48.8	178.0	28.7	20.1	144.3	0.41
11	700	46.1	174.0	27.1	22.4	141.4	0.48
3	750	39.9	155.0	23.0	14.5	130.8	0.36

Average and maximum current magnitudes for the measurement period have been found for all depth cells (**Figure 5** - **Figure 6**). The marked increase in velocity from around 400-500 m depth to the uppermost measurement cell, as seen in **Figure 4**, is further accentuated here. This depth coincides quite well with the starting depth of the relatively homogeneous water mass found in the hydrographic data collected at the same location in August 1999 (Sundfjord et al., 1999). Average currents ranged from 38.7 mm/s at 757 m depth (Cell 2) to 104.3 mm/s at 259 m (Cell 85). Corresponding maximum velocities were 121.0 and 446.0 mm/s, in the same two depth cells. All depth cells had minimum current velocities in the 0-5 mm/s range.

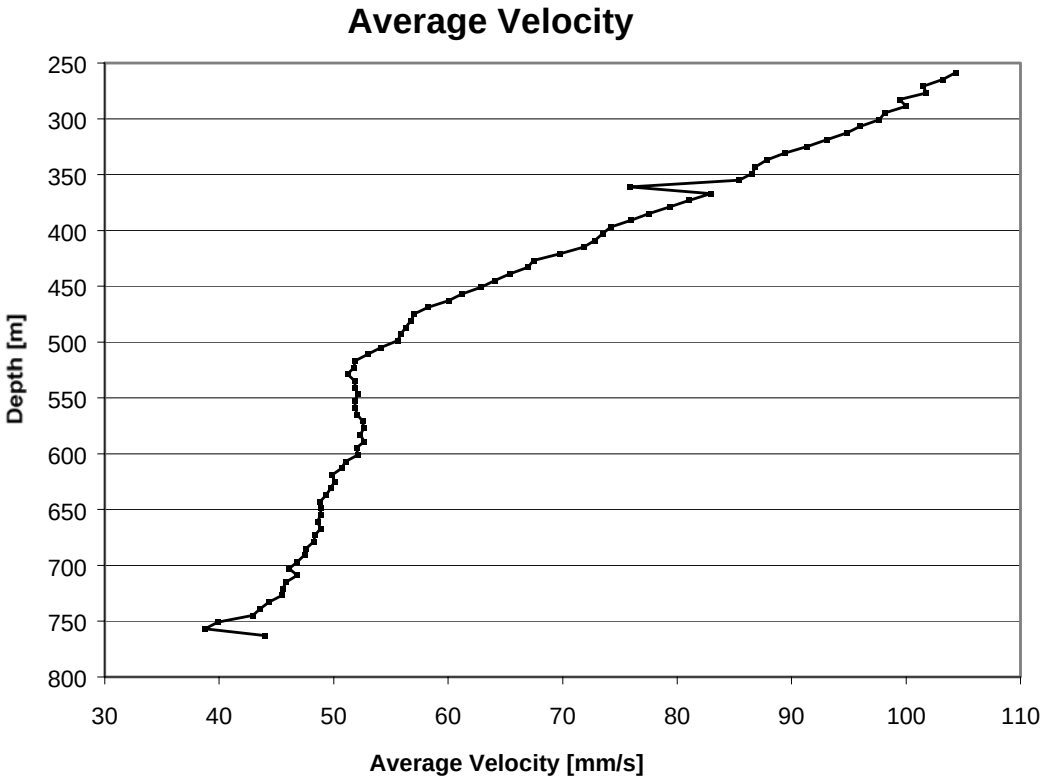

Figure 5. Average ADCP current magnitude for the whole measurement period, for all depth cells.

Cell number 68, centered at around 360 m depth, has a markedly lower average velocity than the surrounding cells. Bearing in mind the depth, and also the long averaging period of more than one month, it is considered unlikely that this local velocity minimum reflects the real physical situation. The spike in the curve could be caused by some sort of reflection of the acoustic signal, either from the steeply dropping seabed or the ocean surface. It could also be an internal numerical artefact. Anyway, the difference between the average velocity of cell 68 and the average of the two cells above and below it is of around 10 %. The values recorded in this particular cell can therefore still be attributed more to the actual currents than to interference by other factors.

Cell 1 shows an increase in average and maximum current magnitude compared with the cells immediately above it. The Aanderaa RCM9 measurements, from approximately 20 meters below Cell 1, show an average velocity of 42.5 mm/s, compared to the 43.9 and 38.9 mm/s of Cells 1 and 2, respectively. Considering the fact that the RCM9 has the shorter averaging period (10 minutes) of the two instruments, one would expect to see higher magnitudes for the RCM9. This leads us to believe that the values recorded for Cell 1 might be somewhat over-estimated. Whether the increase in Cell 1 is an artefact or actually can be attributed to i.e. topographic effects, does however remain somewhat unclear.

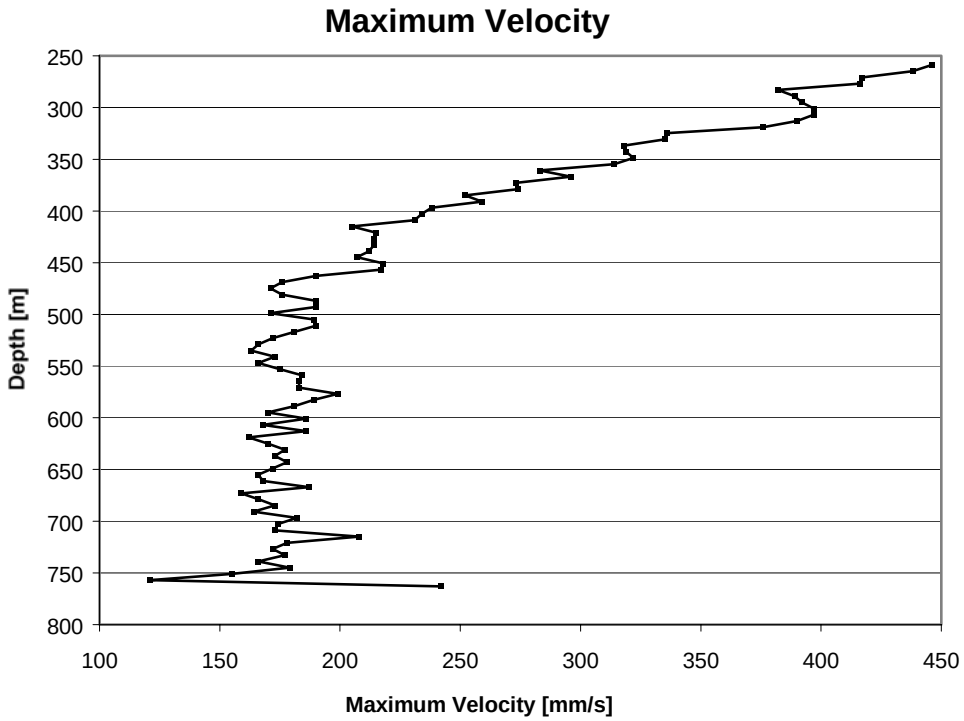

Figure 6. Maximum ADCP current velocity for the whole period, all depth cells.

In Appendix A, plots of current velocity vs. time, current direction vs. time, percentile distribution of current direction and relative flux, mean and maximum velocity in 10 degree sectors, and current velocity distribution (number of recordings in different "classes") are presented for every 50 meters. As an example, the same plots are shown for Cell 1 (763 m) in Figures 7-13.

Time variation of current velocity in Cell 1 is shown in **Figure 7**. All the recorded ensembles for this particular depth interval are included, to show short term variation. In addition, a 24.5 hour moving average has been calculated to remove the tidal signal. There are rapid changes between individual

ensembles throughout the deployment period, whereas the averaged currents show much smaller variation.

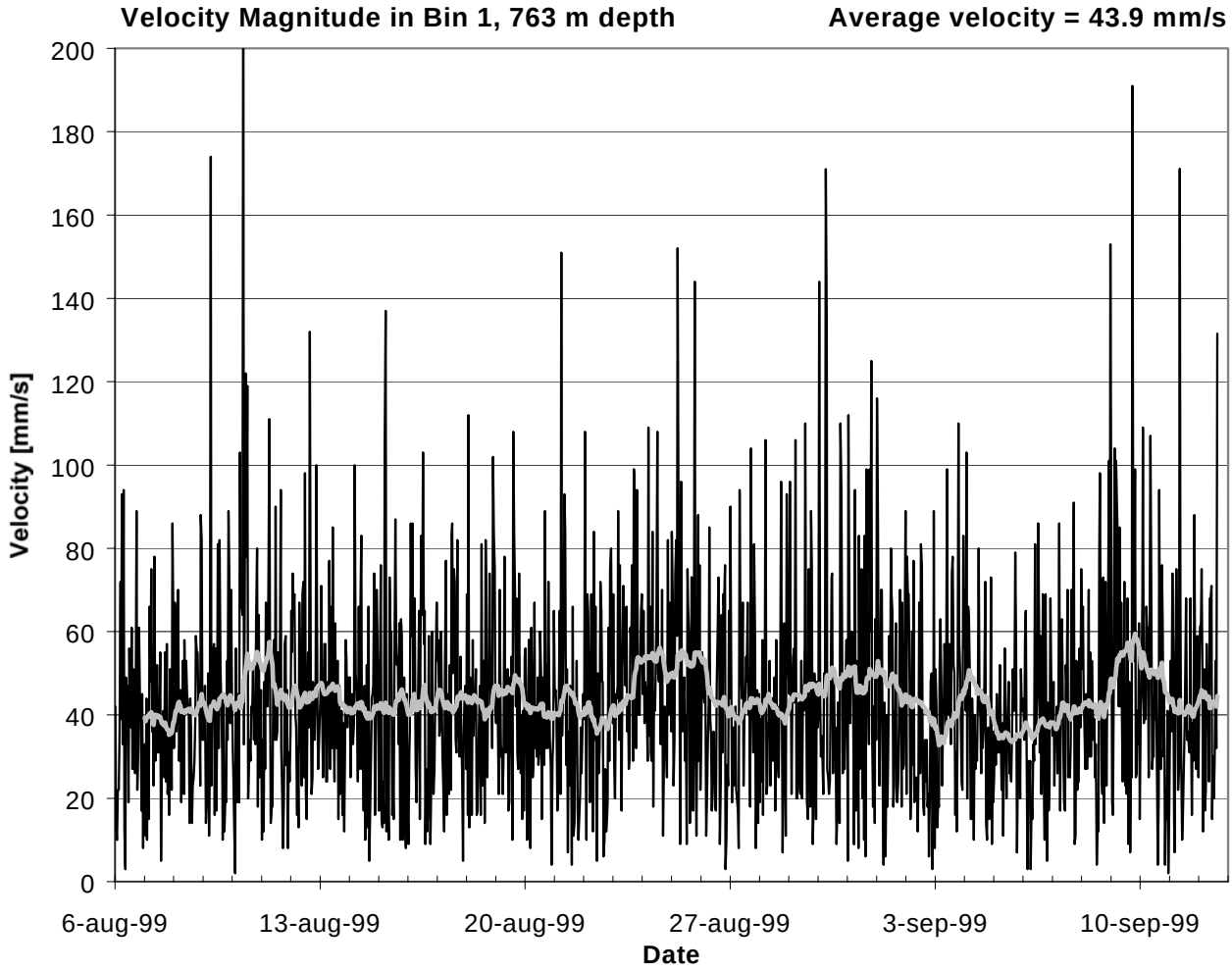

Figure 7. Horizontal velocity magnitude in Cell 1, 763 m depth, for the whole deployment period. The original 40 minute ensembles are shown in black, and a 24.5 hour moving average in gray.

Mean and maximum velocity in different directions for Cell 1 is shown in **Figure 8** and **Figure 9**. At this depth, there is no particular trend as to directions of generally stronger currents. The maximum currents differ much more than the average, but judging by the low number of very high current speed recordings (as seen in the previous figure), this appears to be more coincidential than systematic.

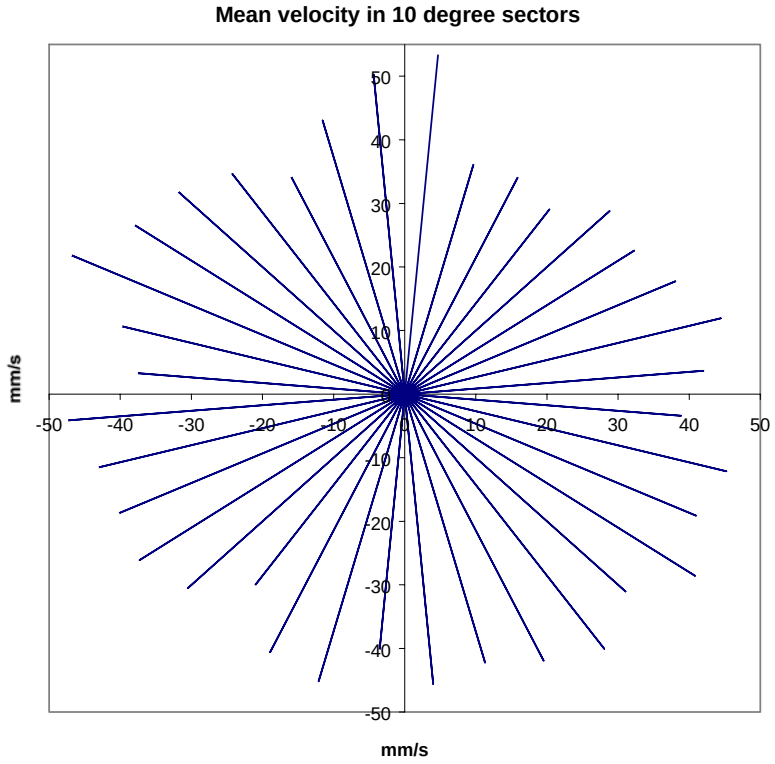

Figure 8. Mean horizontal velocity in 10 degree sectors for Cell 1, August 6 – September 12, 1999.

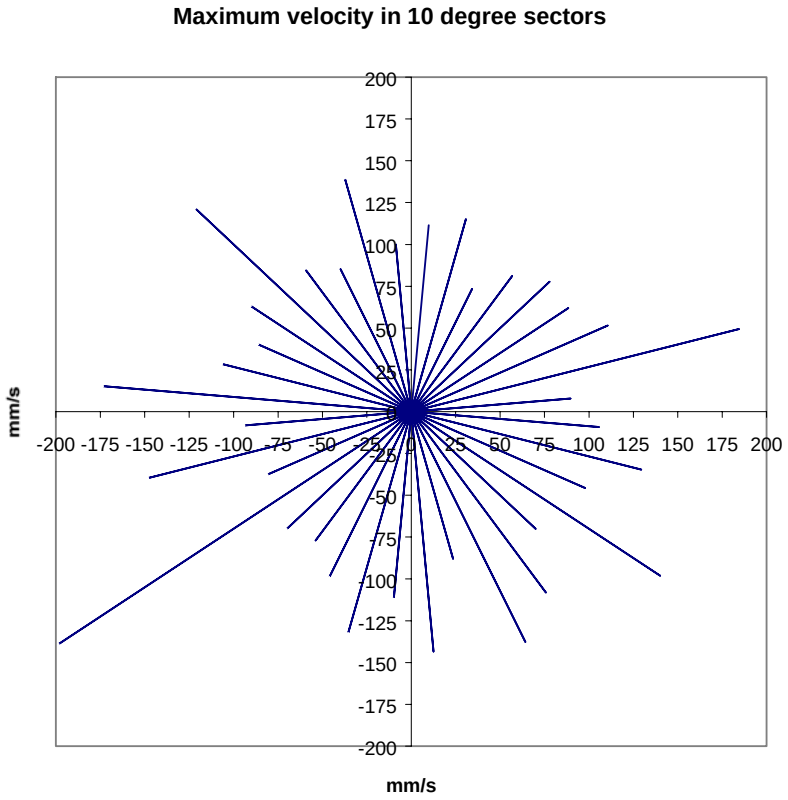

Figure 9. Maximum horizontal velocity in 10 degree sectors for Cell 1, August 6 – Sept. 12, 1999.

Variation of the current direction with time is shown in **Figure 10**. No major shift in the current regime appears to take place in the measurement period. There are no obvious "preferred" current directions at this depth, although there is a certain overweight of recordings in the 90-180 degree area. Approximately 38 % of the recorded current measurements are directed in this 90 degree sector, implying frequent current towards the SE. Around September 1-5 a larger number of the recordings are in a northerly direction. This particular period of time coincides with a change in other depth cells as shown in the Appendix; those with a general NW direction shift towards south and vice versa.

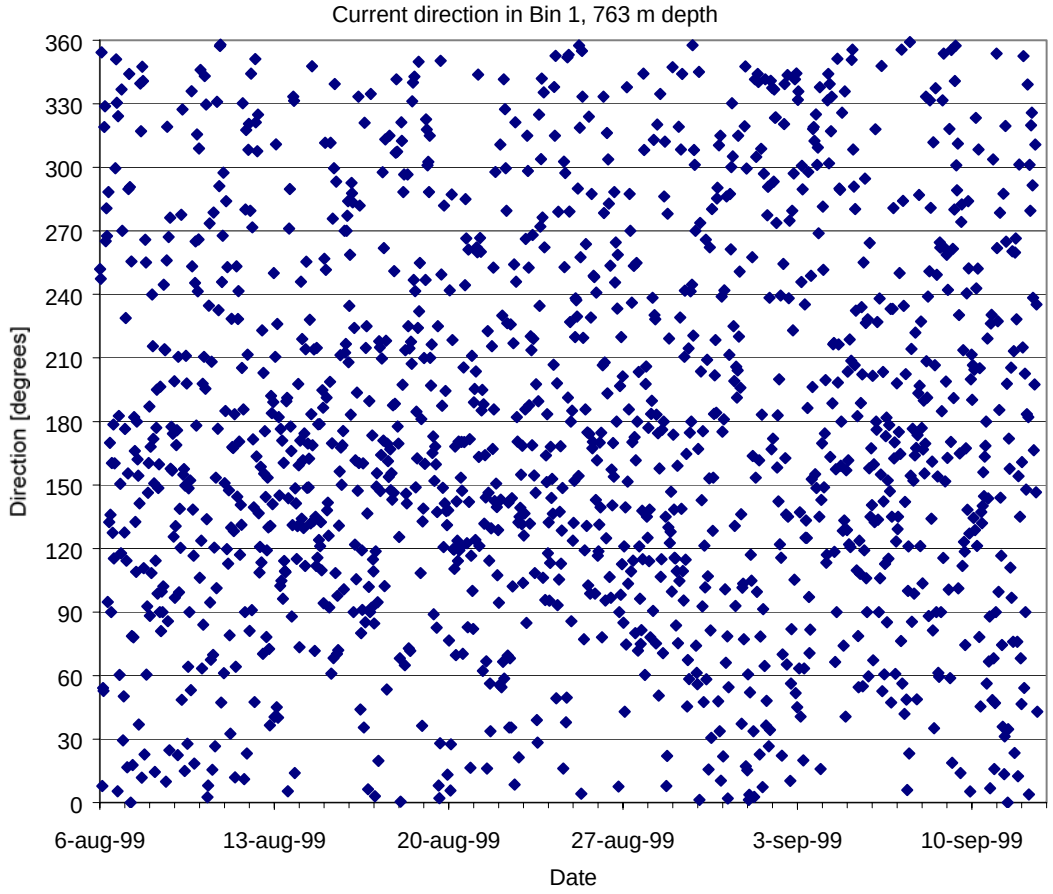

Figure 10. Current direction variation with time in Cell 1, for the whole deployment period.

Figure 11 and **Figure 12** further elaborate how the current direction is distributed. **Figure 11** shows the number of recordings within sectors, while **Figure 12** also takes into account the velocity of each individual measurement, thus yielding the actual amount of water transported ("flux") in each direction. It was shown before that the mean velocity was rather uniform in all directions, so the difference between these two figures is small.

The corresponding figures for directional distribution in Appendix A for other depths show that certain current patterns become more pronounced higher up in the water column. In the intermediate cells directions towards the SE are most common, whereas the current generally goes in a NW direction in the upper cells.

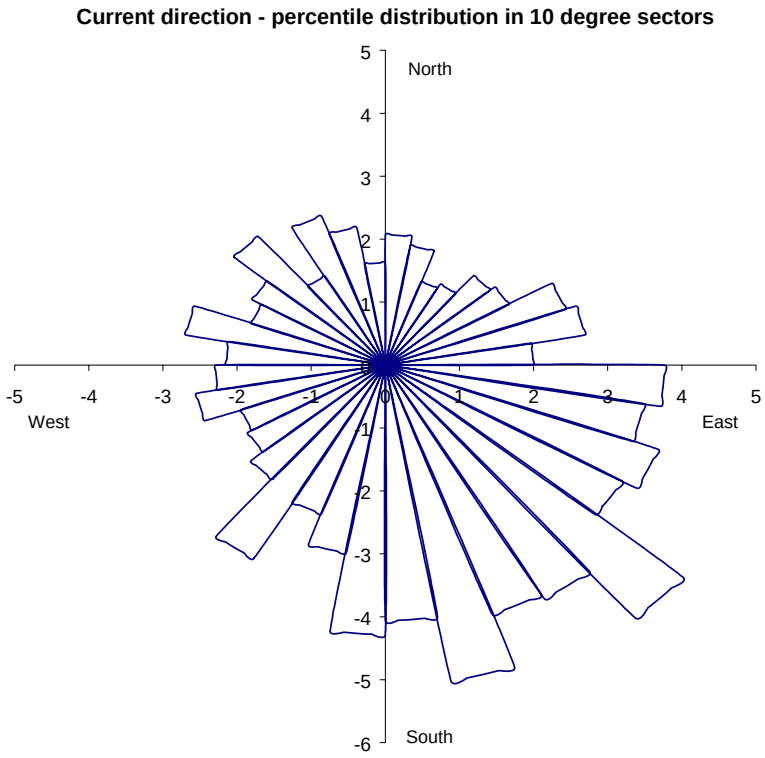

Figure 11. Current direction observations in 10 degree sectors for Cell 1. N is up, E to the right, the values on the axes denote percentage of recordings in each sector.

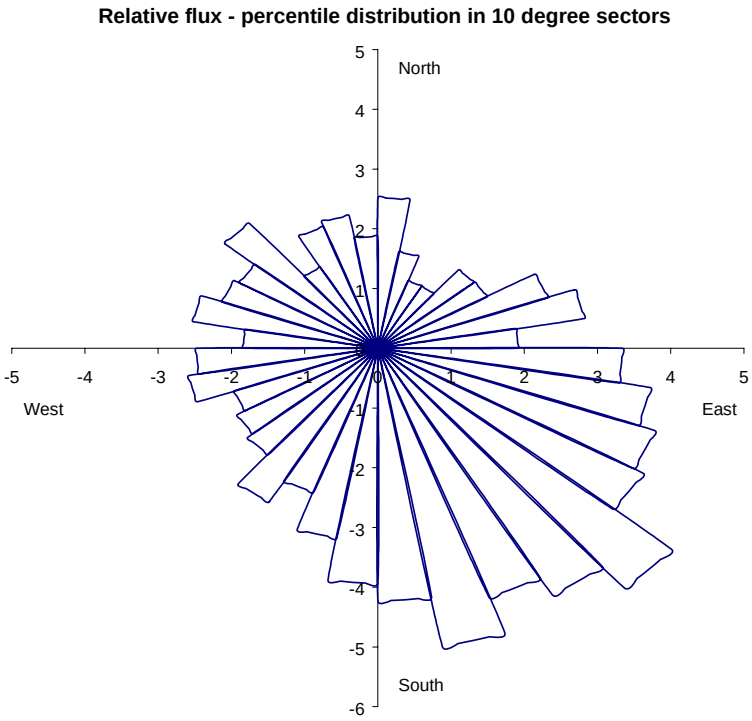

Figure 12. Relative flux in 10 degree sectors for Cell 1. N is up, E to the right, the values on the axes denote percentage of water transport in each sector.

The current velocities have also been distributed in "classes" (**Figure 13**). Close to 75 % of the measurements in Cell 1 have velocities between 10 and 60 mm/s and more than 90 % fall within the 5 to 80 mm/s range.

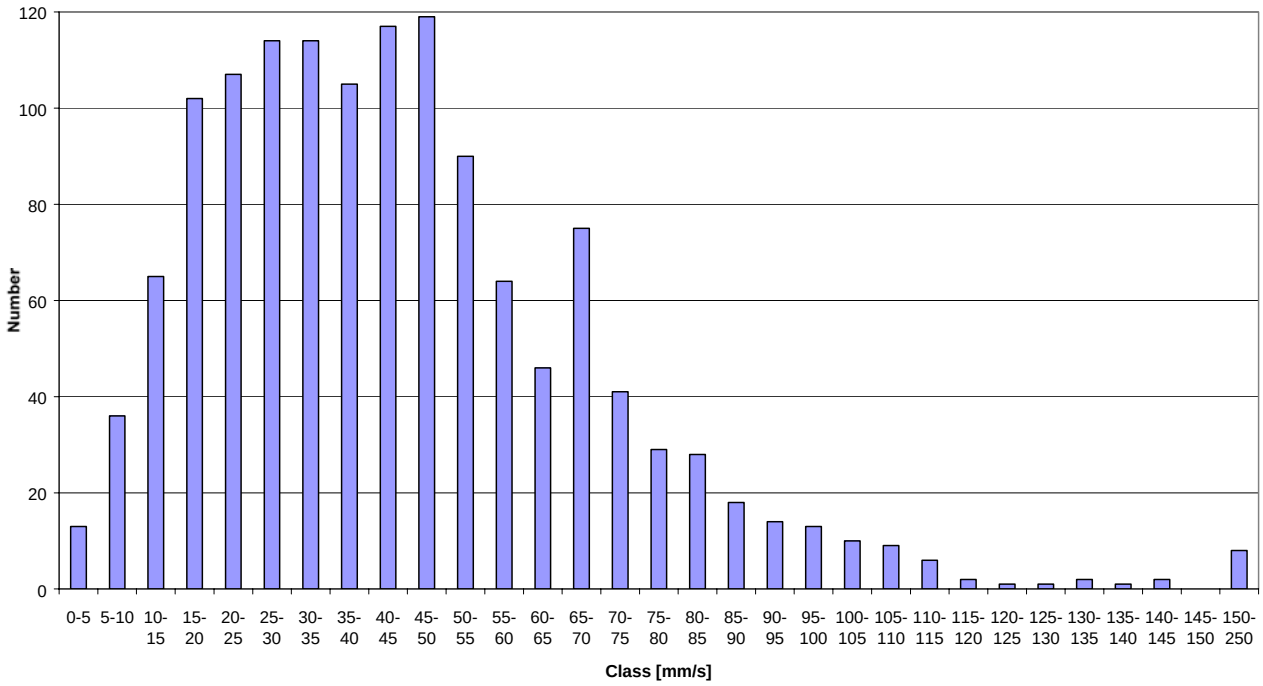

Figure 13. Distribution of current velocities is classes. Cell 1, August 6- September 12, 1999.

3.1.2 Vertical velocities

Vertical velocities are also measured by the RDI ADCP. Vertical water movements were detected in the entire water column throughout the measurement period. **Table 3** shows RMS (Root Mean Square) magnitude of the vertical current, maximum values recorded, and the actual average current for every 50 meters. It can be seen that there appears to be a downward average flux at all depths.

Table 3. Vertical current magnitudes [mm/s] at 50 m intervals.

Cell #	Depth [m]	RMS Vertical Magnitude	Maximum Vertical Magnitude	Average (Net) Vertical Magnitude
85	259	23.6	65.0	-10.3
78	300	14.4	64.0	-10.4
70	350	13.5	62.0	-9.6
61	400	10.2	56.0	-7.9
53	450	5.8	11.0	-4.6
45	500	4.8	13.0	-3.1
36	550	4.7	16.0	-1.5
28	600	5.2	17.0	-2.5
20	650	5.5	18.0	-2.4
11	700	6.3	24.0	-2.0
3	750	6.1	22.0	-1.7

As an example of how the vertical velocity varies with time, the measurements from Cell 1 are shown in **Figure 14**. A 24.5 hour average has been superposed on the actual 40 minute interval values.

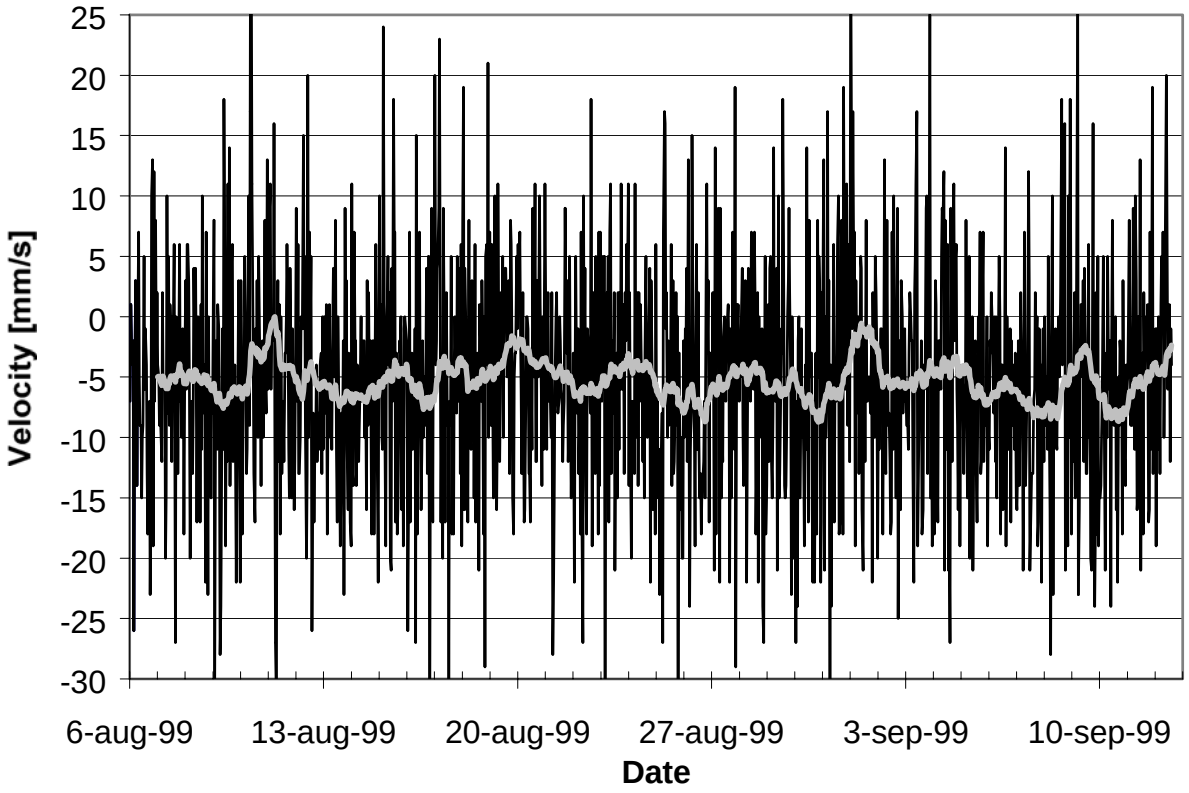

Figure 14. Vertical current velocity vs. time in Cell 1, for the whole deployment period.

3.1.3 Data quality

The instrument calculates the speed of sound, C, automatically, using the following formula: C_{real} = 1449.2 + 4.6T - 0.055T^2 + 0.00029T^3 + (1.34 - 0.01T)(S - 35) + 0.016D, where T is temperature, S is salinity and D is depth at the transducer face. Temperature (from the ADCPs built-in thermometer) and depth (from the pressure sensor) are automatically incorporated into the instrument's internal calculation algorithms. A fixed value for salinity is programmed before the deployment starts, and can be corrected during post-processing of the data. In this case, salinity was given a priori as 35.00. Using an average depth of 780 m in the equation above, the speed of sound is found to be 1484.03 m/s. Average salinity at 800 m from CTD data acquired during the August 03-08 'KOK' cruise (Sundfjord et al. 1999) was found to be 34.45, yielding a C_{real} of 1483.24 m/s. The discrepancy between the CTD and a priori salinity values thus introduces a difference between the recorded ADCP current velocities and the "real" ADCP velocities of about 0.05 %. The salinity also varied throughout the current measurement period. The Aanderaa RCM9 salinity values showed a difference between minimum and maximum of 0.19 (the uncalibrated RCM9 values seemed to be higher than those measured with the CTD, but the measured variability is expected to be real). In this context, such small salinity discrepancies are considered to be of little importance.

The ADCP compass was not recalibrated on board the ship after installing new batteries and assembling the steel frame. The measured main current directions do nevertheless seem to be in good accordance with local topography, and the lower cells show similar directional statistics as the RCM9 just below.

To evaluate the quality of the data obtained by the ADCP, the correlation between the received return signal and ambient (background) noise was analyzed. This correlation, as given by RD Instruments, is 128 when the signal to noise ratio is high, and the threshold value is set to 64 (the level where background noise dominates the signal received by the ADCP). All depth cells in the Keahole Point deployment have average correlation values above 105, and about 70% of the cells have average correlation values between 125 and 131. This time-averaged correlation for the different depth cells is shown in **Figure 15** below. The correlation decreases with distance from the instrument, as the acoustic signal is depleted. Note also the spike in cell 68, which was commented on earlier in this chapter. Another feature is the relatively low values near the instrument. This could be caused by slope reflections, or simply be due to difficulties in decoding the sound signals that have the shortest travel time relative to the transducers. Nevertheless, all depth cells have average correlation values well above the limit of 64.

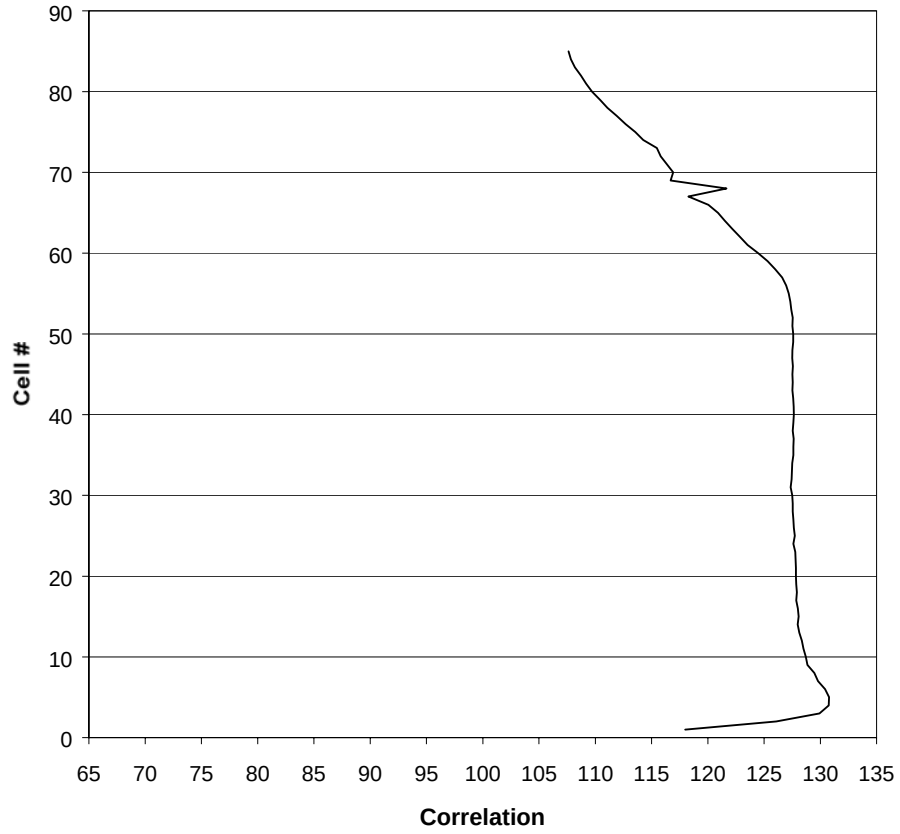

Figure 15. Correlation between the ADCP return signal and ambient noise for the different depth cells, averaged over the whole deployment period. The lower threshold for good quality data is 64.

3.2 Aanderaa RCM9

The Aanderaa RCM9 made valid measurements from 00:10 August 6 to 23:00 September 12. The total number of recordings in the period was 5466. Average current velocity throughout the measurement period was 4.25 cm/s, and the maximum speed was 14.67 cm/s. The measurements are presented in the same formats as the data from RDI ADCP Cell 1 in Para. 3.1.1. The variation with time of the original 10 minute interval current velocities is shown in **Figure 16**, along with a 24.5 hour moving average. Average and maximum velocities in different directions are plotted in **Figure 17** and **Figure 18**. Current direction vs. time is plotted in **Figure 19**, and current direction and flux in different sectors in **Figure 20** and **Figure 21**. The distribution of current velocities in different classes is found in **Figure 22**.

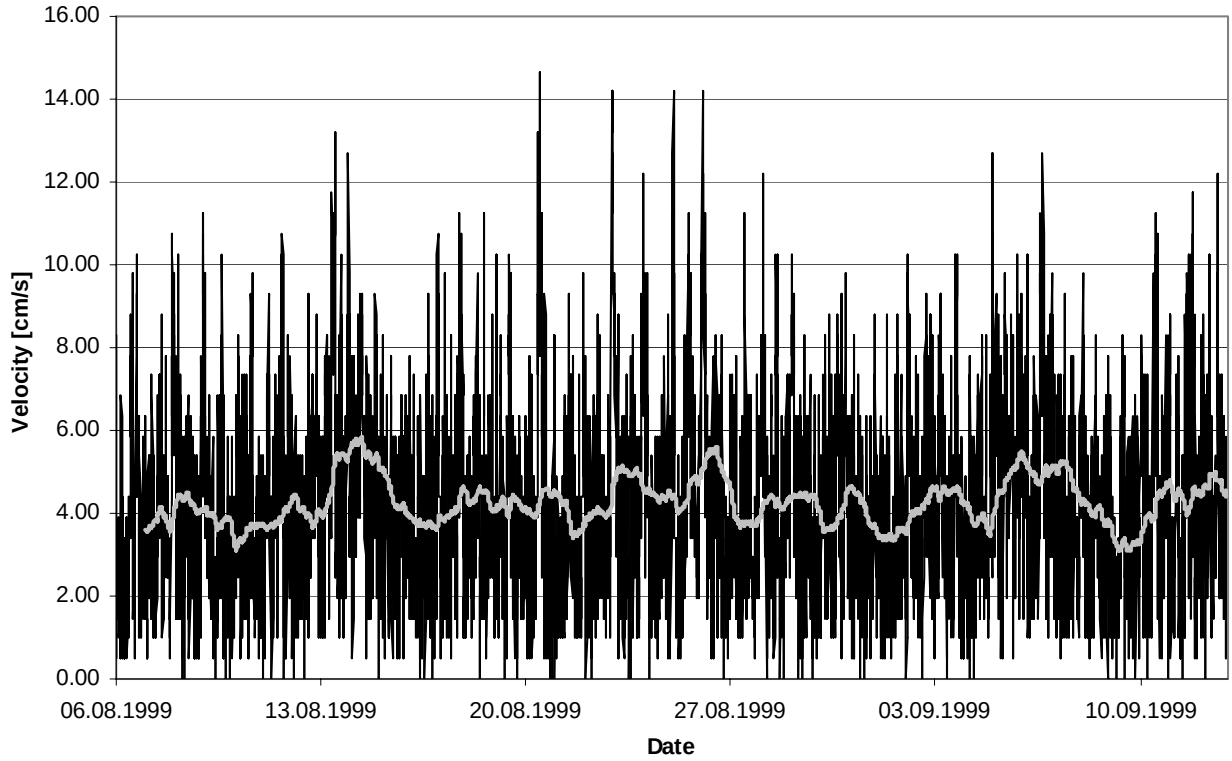

Figure 16. Current velocity as measured by the Aanderaa RCM9, August 06 – September 12, 1999. Ten minute interval recordings in black, 24.5 hour moving average in gray.

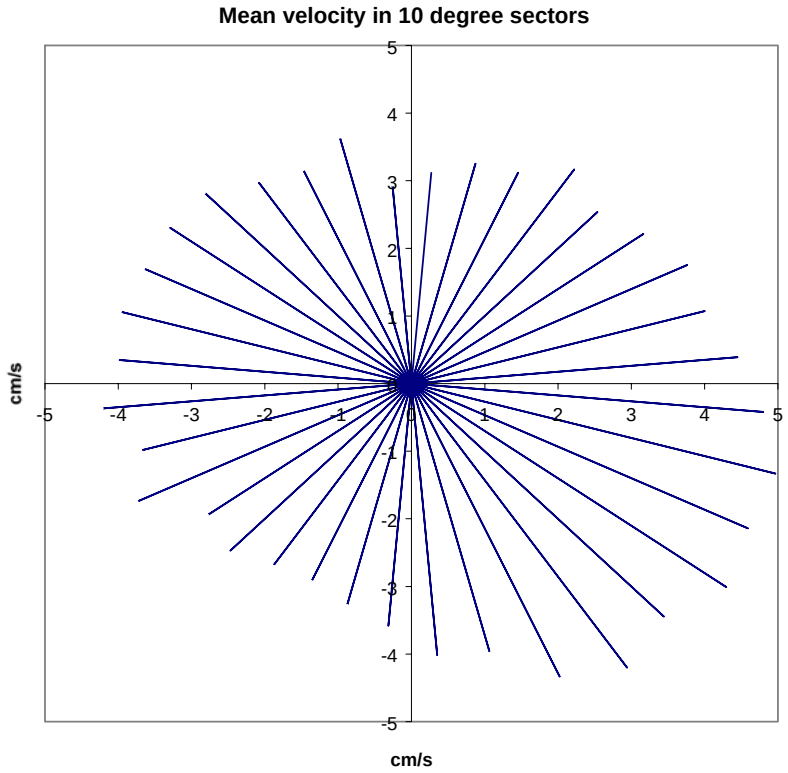

Figure 17. Mean current velocity distribution in 10 degree sectors for the Aanderaa RCM9.

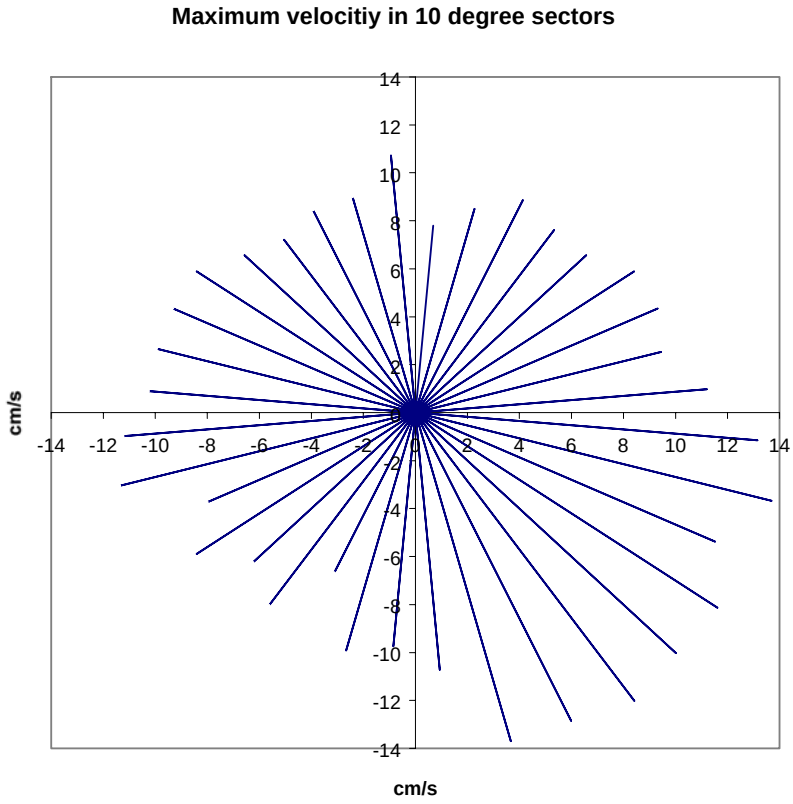

Figure 18. Maximum current velocity in 10 degree sectors for the Aanderaa RCM9.

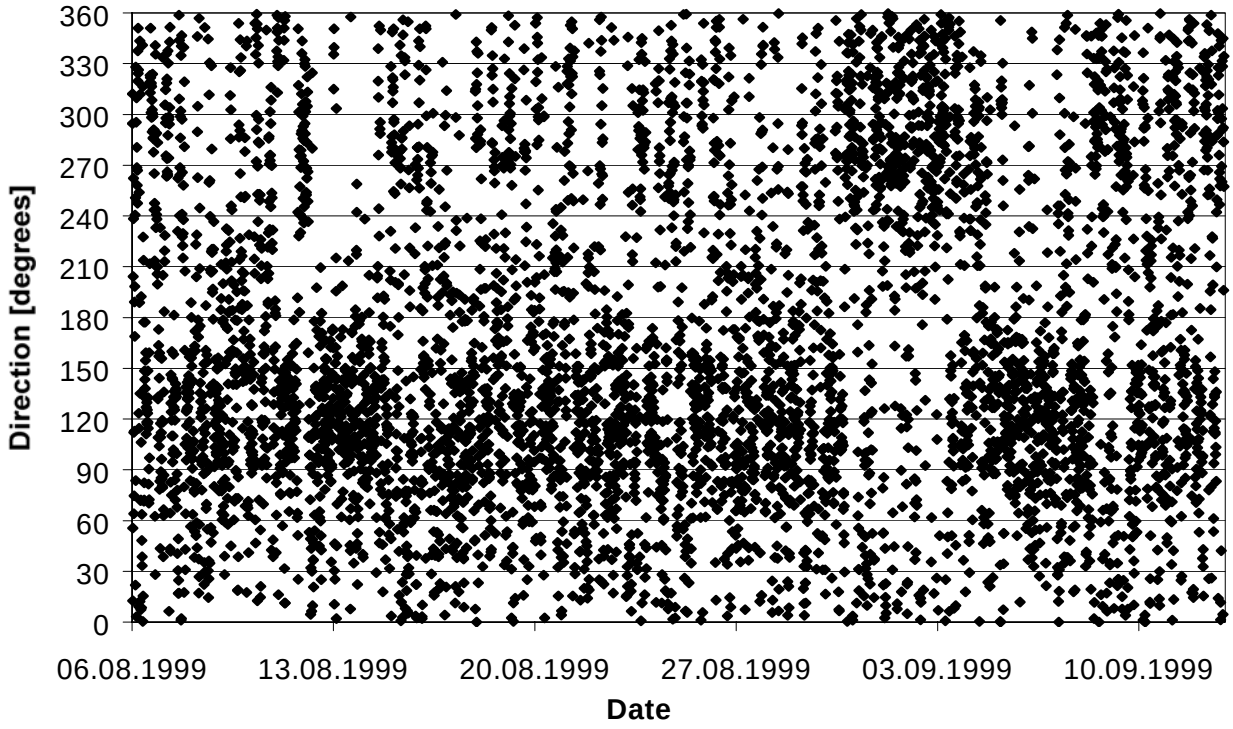

Figure 19. Current direction vs. time as measured by the Aanderaa RCM9.

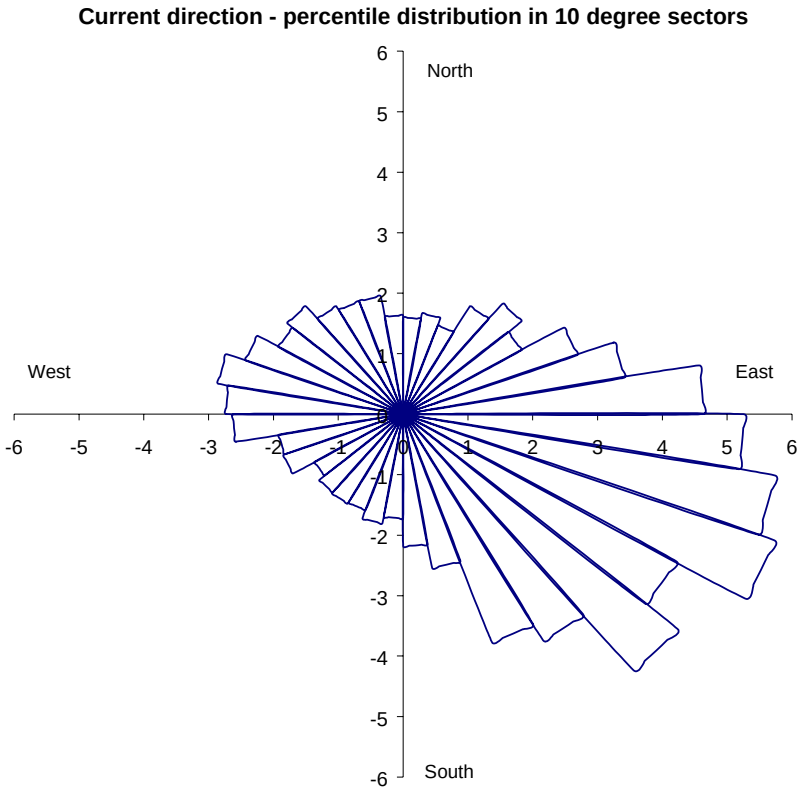

Figure 20. Current direction in 10 degree sectors for the RCM9.

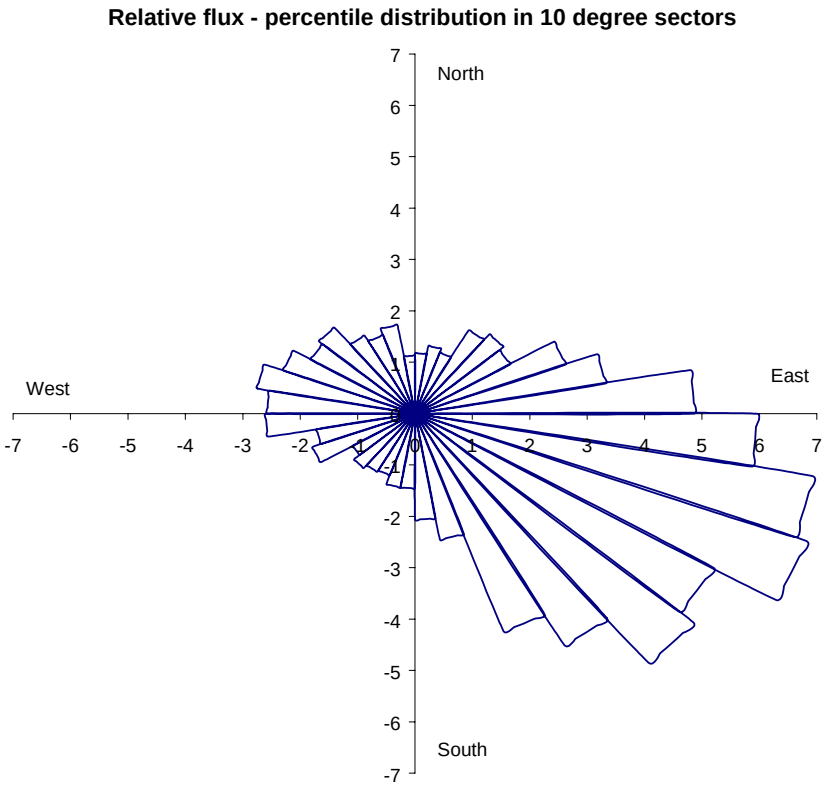

Figure 21. Relative flux in 10 degree sectors for the RCM9.

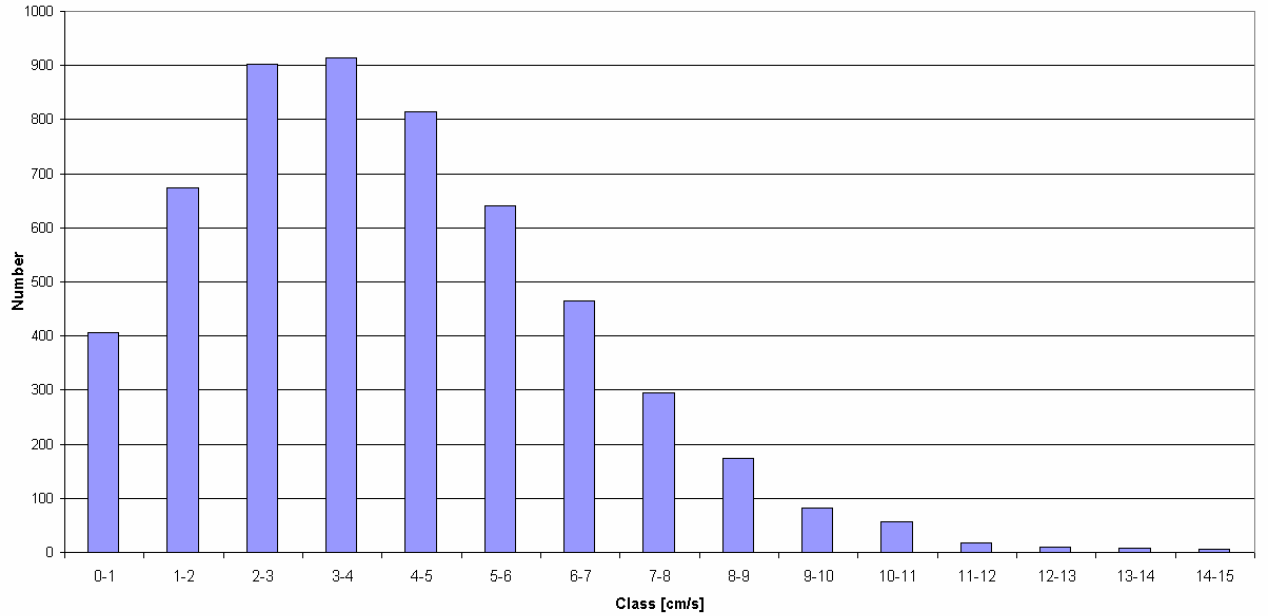

Figure 22. Distribution of current velocities in classes for the RCM9 data.

The RCM9 was also equipped with a turbidity meter. There are not many particles in the deep water in this part of the Pacific Ocean, and this was reflected in the low values and moderate variation recorded with the RCM9. Average turbidity for the August-September deployment was 0.21 NTU (Nephelometric Turbidity Units - see Mylvaganam and Jakobsen, 1999), whilst the maximum was found to be 0.33 NTU.

Temperature and conductivity (which is converted into salinity) were also recorded by the Aanderaa RCM9, at 10 minute intervals. Variation of these two parameters at the instrument depth was small throughout the period – see **Table 4** for details on average and extreme values, and **Figure 23** - **Figure 24** for time series plots.

Table 4. Statistical values for temperature and salinity from the RCM9 measurements, August 6-Sept. 12, 1999.

Temperature*	**[ºC]**	**Salinity****	**ppt**
Average	5.18	Average	35.30
Maximum	5.65	Maximum	35.37
Minimum	4.81	Minimum	35.18
Δ temperature (range)	0.84	Δ salinity (range)	0.19

* Average temperature from the RDI ADCP in the same period was 5.15 ºC.

** Average salinity in the CTD casts 4-6 August close o the bottom was 34.45, implying that the RCM9 values probably are ~ 0.8-0.9 too high.

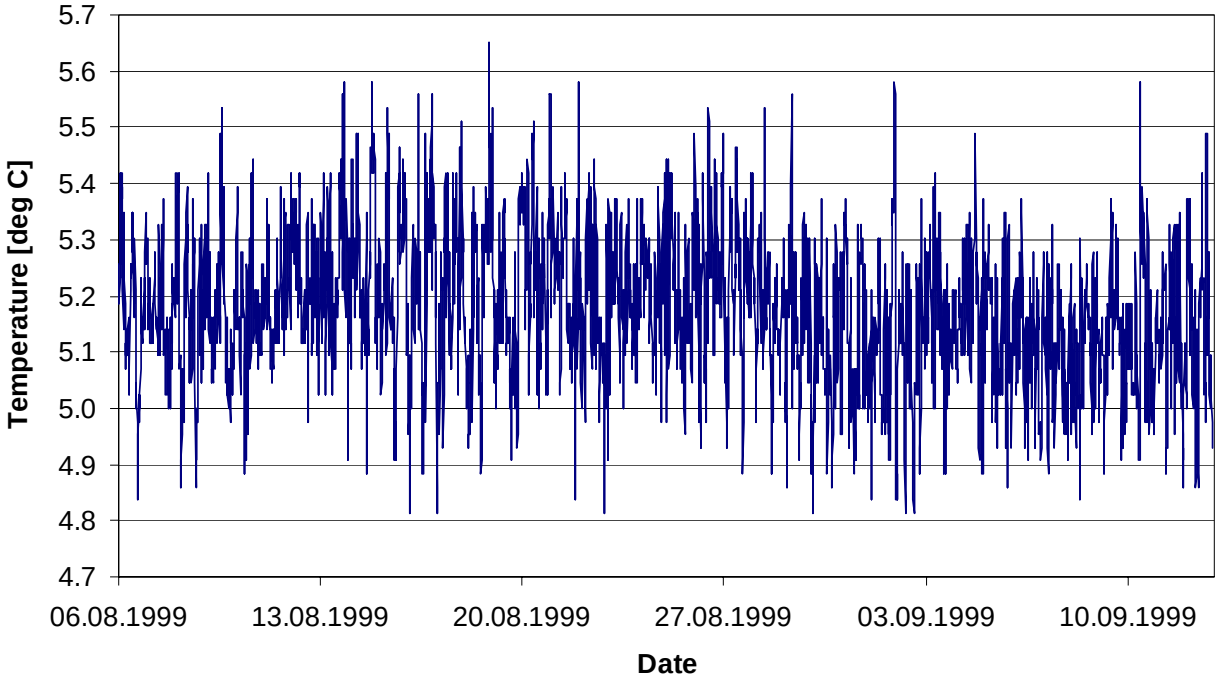

Figure 23. Temperature measured by Aanderaa RCM9, August 06 – September 12, 1999.

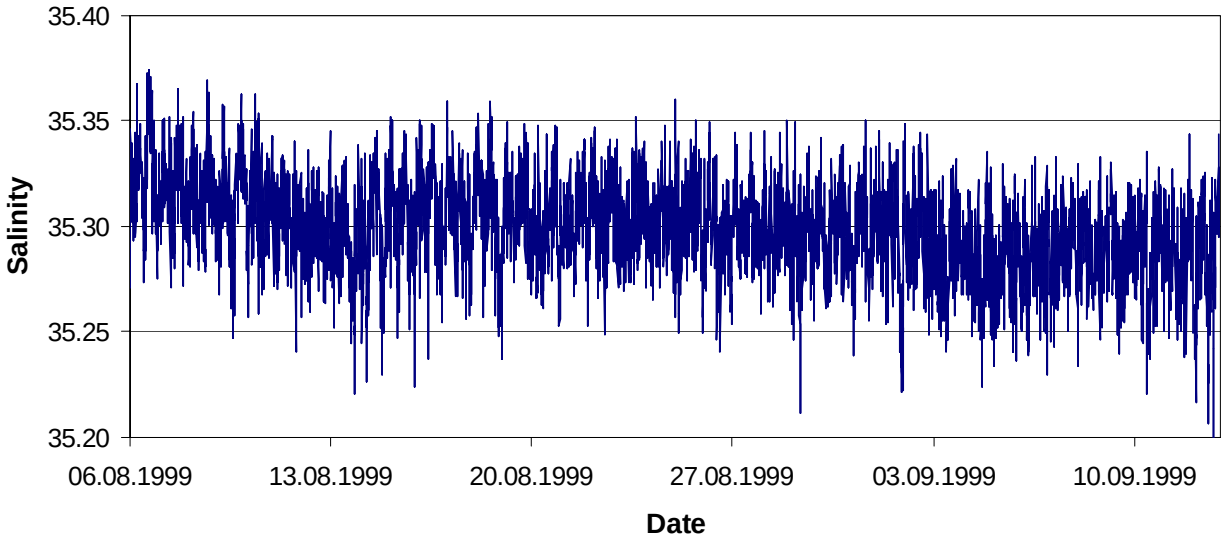

Figure 24. Salinity measured by the Aanderaa RCM9, August 06 – September 12, 1999. The values are probably ~ 0.8-0.9 to high, according to CTD measurements made prior to the deployment.

4. Analyses and discussion

4.1 General remarks

The collected data are sparse in time and spatial coverage, but it must be anticipated that the current measurements do reflect features of a general and known character that to some extent have been described previously. Flament at al. (1996) described the general currents and hydrographic conditions in the Hawaiian waters. Surface waters are warm, with a rather strong north to south gradient, but with small annual cycles. Also, temperatures tend to be higher west of the island chain. The highest temperatures are found in September (average 27 ^{o}C around O'ahu), lowest in March (average 24 ^{o}C at O'ahu). The average surface salinity is at a maximum at 26˚N (35.2 ppt), gradually declining to about 34.3 ppt at 10˚N.

The winds mix the upper part of the water column. The depth (thickness) of this mixed layer typically ranges from 120 m in winter to less than 30 m in summer. The thermocline starts at the bottom of this layer, with temperatures gradually decreasing from around 20 ^{o}C to about 5 ^{o}C at 800 m (about the maximum depth we are concerned with), and further to about 1.5 ^{o}C at the deep bottom, beyond the depths of our interest in this project.

Large-scale currents below the surface layer are probably mainly geostrophic, but partly modulated along the island by the tides. The main flow direction in this region is from east to west. Surface currents are highly influenced by winds and air pressure fields, forming rather complicated flow patterns with many local features. South of Hawaii average westward surface currents are about 17 cm/s, while on the north side of Hawaii averages are near 25 cm/s. Below 1000 m depth, the geostrophic currents are generally less than 5 cm/s, but their patterns are not entirely known (Flament et al. 1996).

We already described the general current magnitudes and directions obtained from the summer 1999 measurements. In this chapter, a few topics of particular relevance to the CO_2 sequestration project are investigated more closely. For designing an optimum monitoring program, knowledge about the current and it's variation is important. For the ROV operators and the personnel involved with the positioning of the CO_2 pipe, vertical shear is also of concern. The numerical modellers might have a particular interest in vertical velocities as well.

4.2 Horizontal currents

The results from the ADCP measurements shown in Para. 3.1 and the Appendices reveal a fluctuating current field. As mentioned earlier, there is a marked difference between the upper part of the measurement range (about 260 – 500 m) experiencing relatively strong NNW currents, and the lower part, where currents are more moderate and generally directed towards the SSE. To illustrate how an imaginary particle would be advected by the current, Progressive Vector diagrams have been produced for some depth cells; Cell 3 near the bottom (in the SSE regime, 750 m depth), Cell 45 in the transitional layer (500 m), and Cell 78 (300 m), well into the upper, NNW-moving portion of the water column. In **Figure 25**, all the current recordings from each cell have been multiplied with the corresponding 40 minute interval, and added together. The net transport differs significantly with depth. In the uppermost cell the total distance covered in the measurement period is 300 km and the net displacement is 139 km to the NNE. The distance covered in Cell 45 is 167 km, but the net movement is only14.4 km. This is to a large extent due to the frequent changes in direction at this depth, with currents in opposite directions that cancel out in these calculations. At 750 m the currents

are weaker on the average, but more unidirectional towards the SSE. Total travel distance here is 119 km, and net movement 47 km. Statistical values from the calculations are shown in **Table 5**.

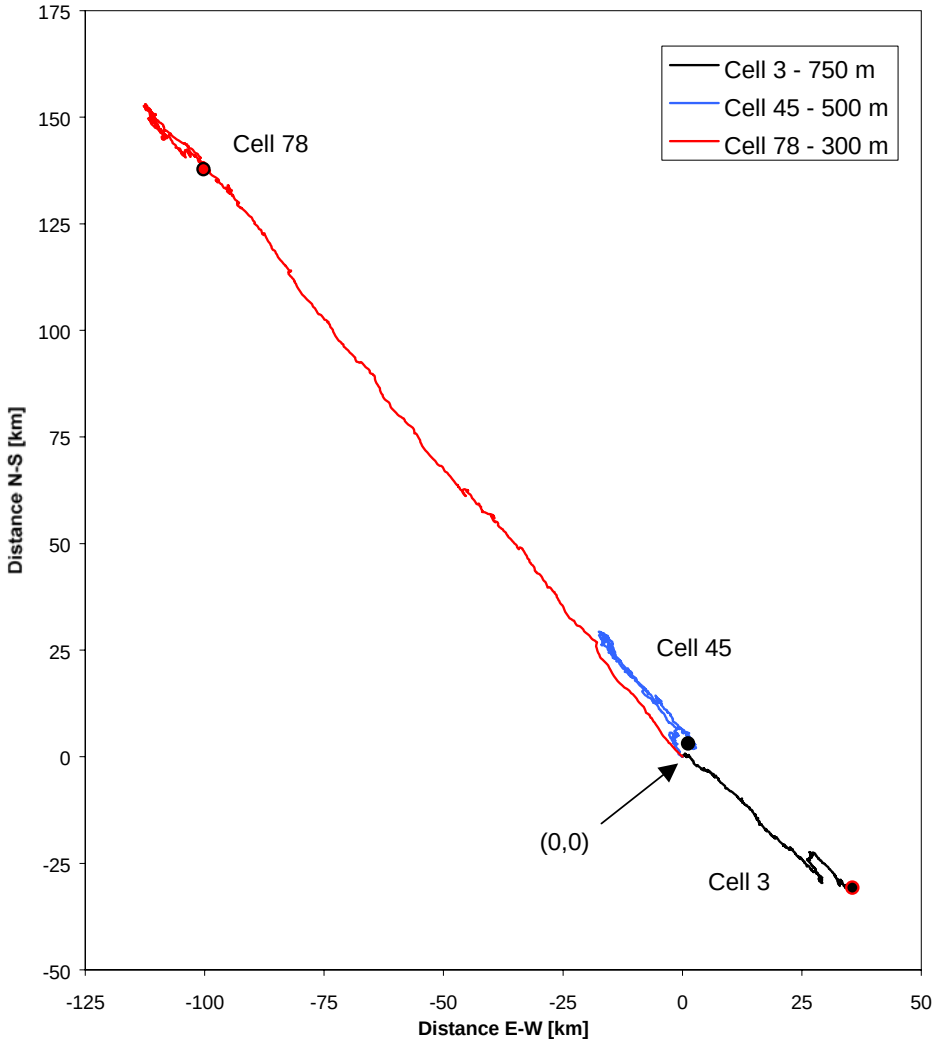

Figure 25. Progressive vectors for Cells 3 (750 m), 45 (500 m) and 78 (300 m). (0,0) shows the starting point, and the circles denote "end-points" for the different trajectories.

Table 5. Statistical values for advection in Cells 3, 45 and 78 from the RDI ADCP.

	Cell 3, 750 m	Cell 45, 500 m	Cell 78, 300 m
Average Velocity	4.0 cm/s	5.6 cm/s	9.8 cm/s
Residual Speed	1.5 cm/s	0.1 cm/s	5.2 cm/s
Net advection/hour	55 m	4 m	190 m
Net advection/day	1300 m	90 m	4500 m
Net advection/week	9.2 km	0.6 km	31.4 km

4.3 Profiles and vertical shear

Figure 26 and **Figure 27** show the measured current speed for all depth cells for six different recording ensembles which are distributed throughout the measurement period by about 5 days separation. The ensembles are otherwise randomly selected and do hardly represent extreme cases. Significant vertical shear from 500 m and up seems to exist most of the time. There is also significant variation with time, and speed maxima are found at varying depths.

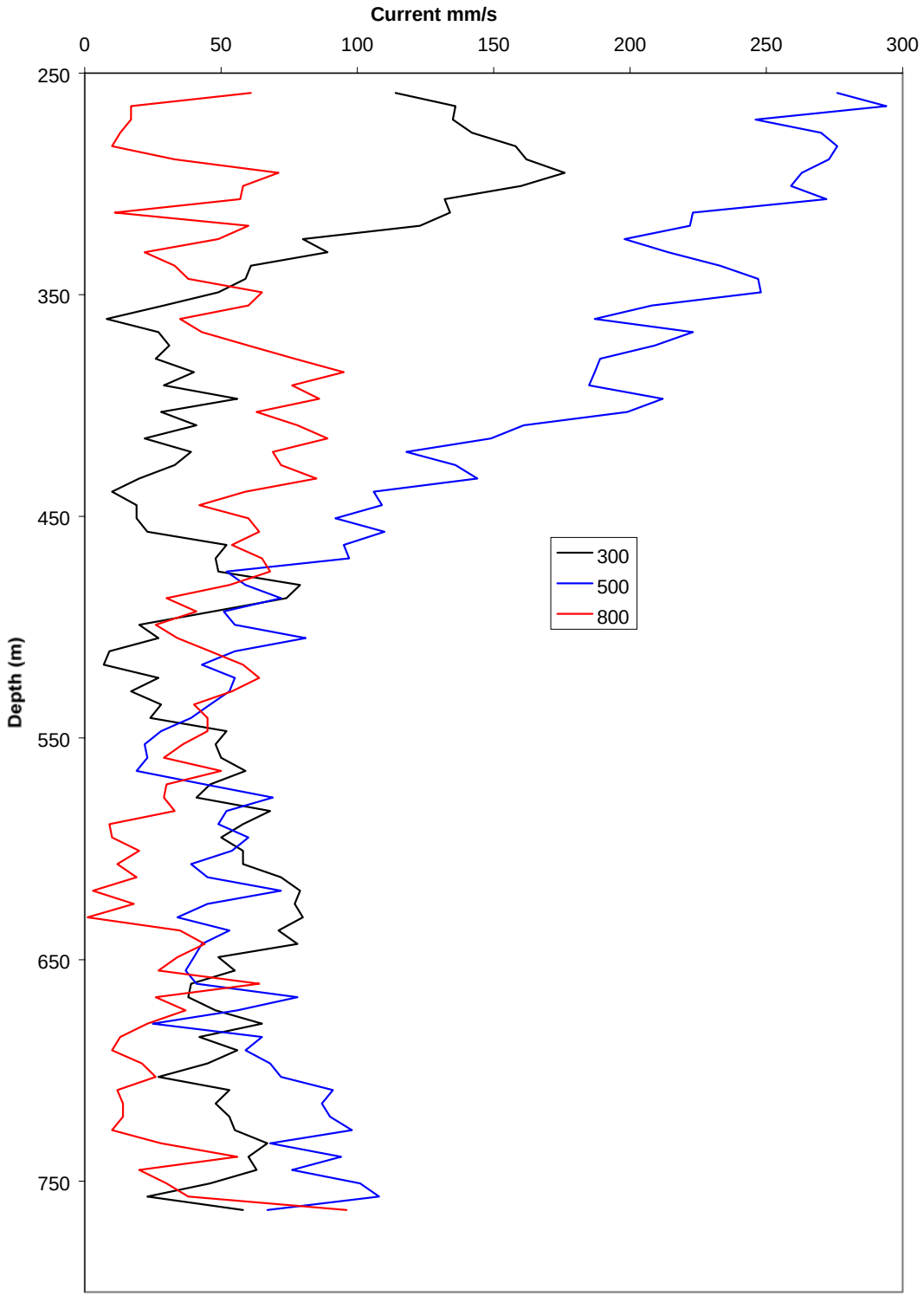

Figure 26. Plots of measured current speed by the ADCP for the ensembles 300, 500 and 800.

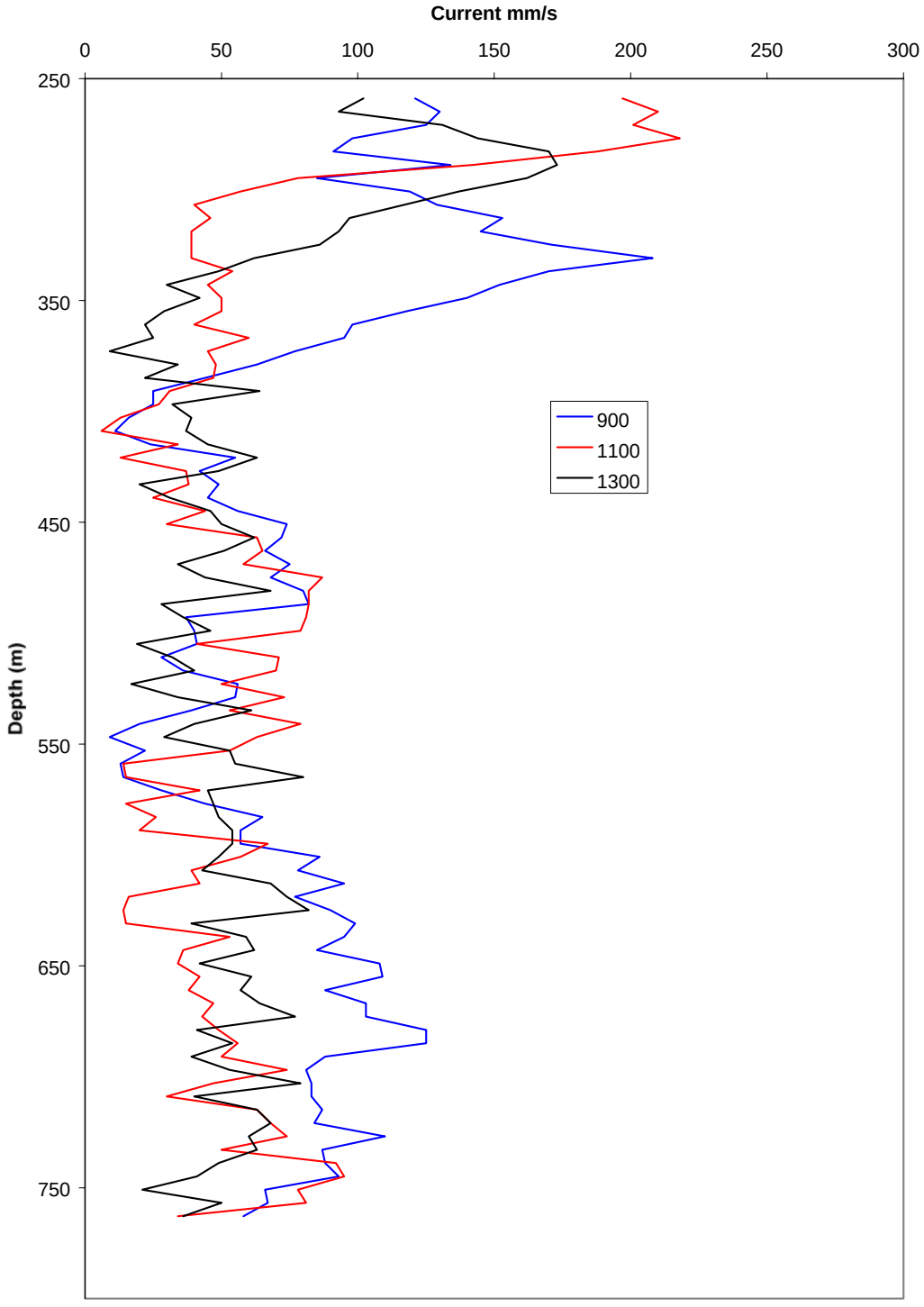

Figure 27. Plots of measured current speed by the ADCP for the ensembles 900, 1100 and 1300.

We have compared two neighbouring cells over a 48 hour period to try to exemplify how large the vertical shear can be. Horizontal current magnitude for Cells 3 and 4 are shown in **Figure 28**, along with the difference between them. The difference has been calculated by decomposing the velocities from Cells 3 and 4, thereby also taking any differences in direction into account. Average shear for this period was calculated to 0.0043/s, and the maximum value found was just over 0.017/s.

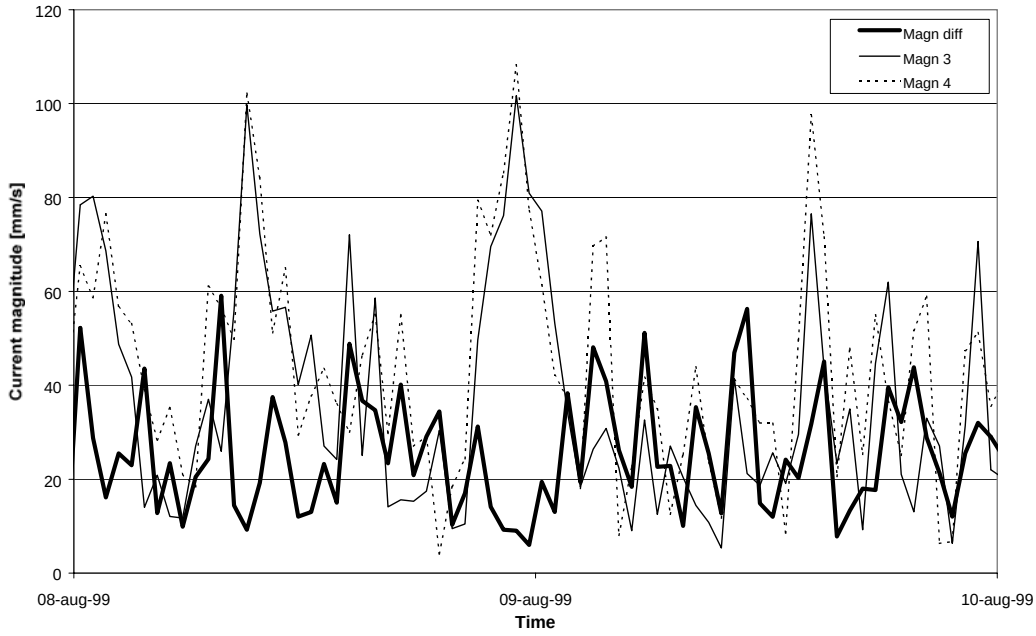

Figure 28. Horizontal current magnitude in Cells 3 and 4 for a two day period, and the difference between them (bold line). The latter is corrected for any directional differences between the cells.

4.4 Vertical velocities

The vertical current magnitudes in **Table 3**, Para. 3.1.2, showed an increase in the cells from 400 m and up. In particular, the maximum values were greater than we would expect from regular dynamic forcing. Plots of vertical velocity vs. time for these cells showed abrupt spikes in the magnitude of the vertical current throughout most of the measurement period (see Cell 78, **Figure 29**).

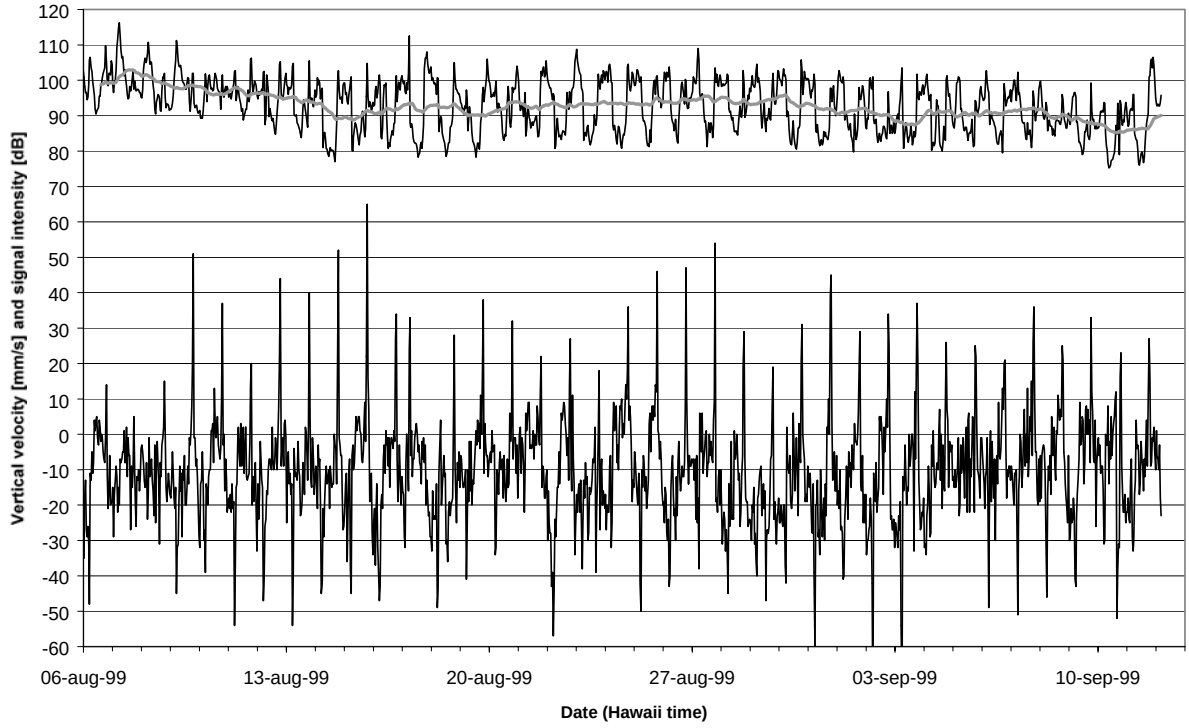

Figure 29. Vertical velocity (bottom) and signal strength (top) vs. time in Cell 78 (300 m), August 06 – September 12, 1999. Gray line shows 24.5 h moving average for signal strength.

Closer examination of shorter time periods revealed that these velocity shifts occur at almost exactly the same times every day; strong upward motions at around 1900 hours (local time) and downward at 0500 (**Figure 30**). These periods of strong vertical velocities usually lasted less than one hour, with magnitudes several times greater than those observed the rest of the time.

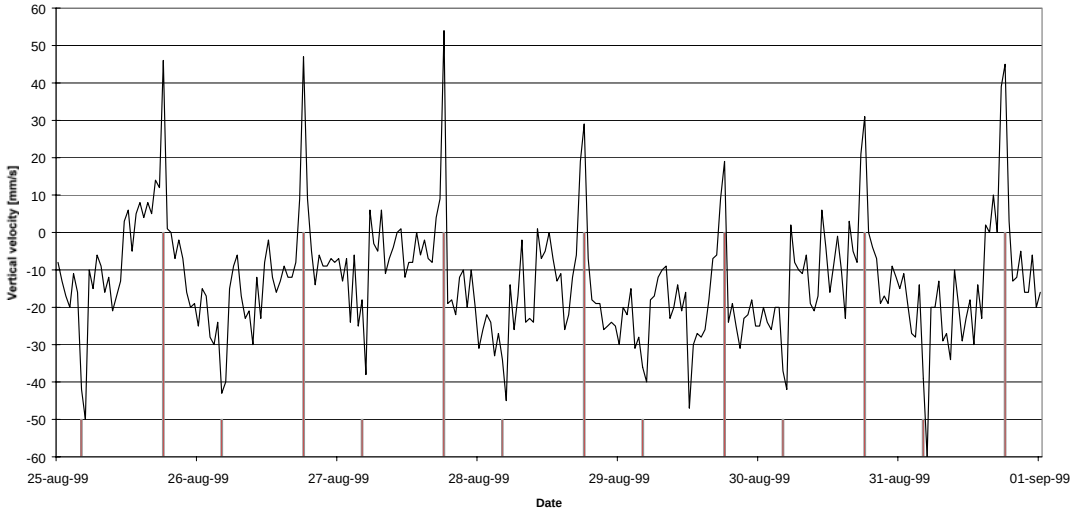

Figure 30. Vertical velocity variations in Cell 78 (300 m) from 25 August – 01 September 1999. Solid bars going to zero denote 1900 hours (local time) and the bars going to -50 denote 0500 hours.

The ADCP actually measures particle movements in the water, and not necessarily the water currents per se. This leads us to believe that the observed jumps in vertical velocities at depths from 250 – 400 m depth are due to migrating zooplankton instead of actual water motion. This assumption is backed by similar observations made elsewhere, where zooplankton rise just around sunset and travel back down at dawn (Rippeth & Simpson, 1998). According to litterature, a maximum in zooplankton distribution is found at 250 – 350 m depth in the Eastern Pacific (Parsons and Takahashi, 1977). The strength of the return signal received by the ADCP is an indicator of the amount of reflecting material in the water. It can be seen from these data that there are less particles in the layers from 250 ~ 400 m during the day, and more at night (i.e. Cell 78, **Figure 31**).

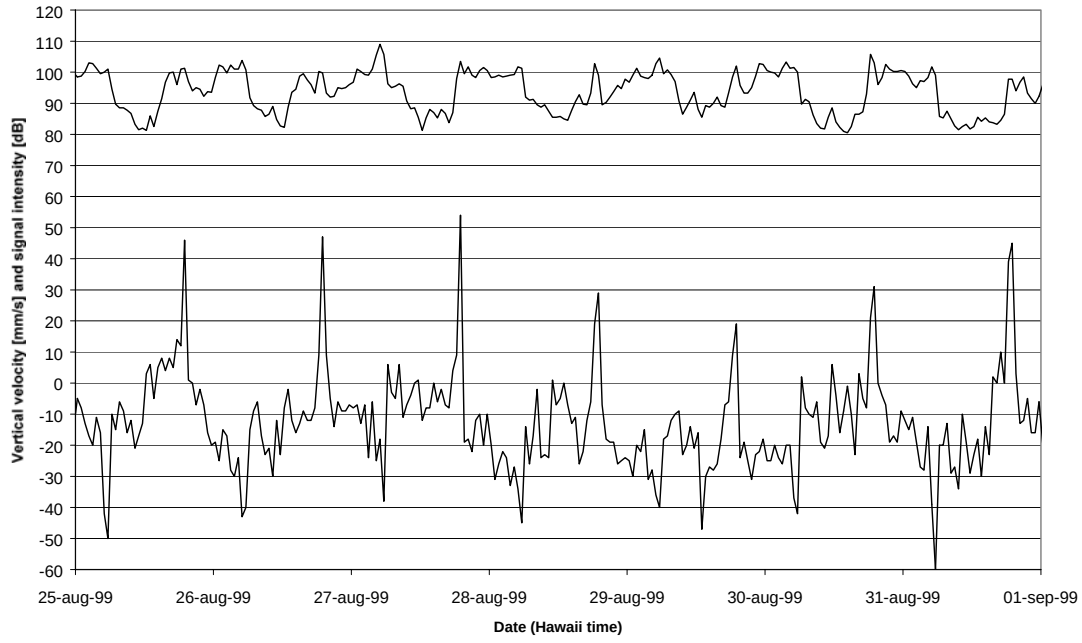

Figure 31. Signal strength (upper line) and vertical velocity (Cell 78) 25 August – 01 Sept., 1999.

Figure 32 shows signal strength distribution from 260 – 470 m for one ensemble recorded during the day (solid line) and one from after nightfall (dotted line). It seems clear that more reflectors are present in the upper part at night and vice versa.

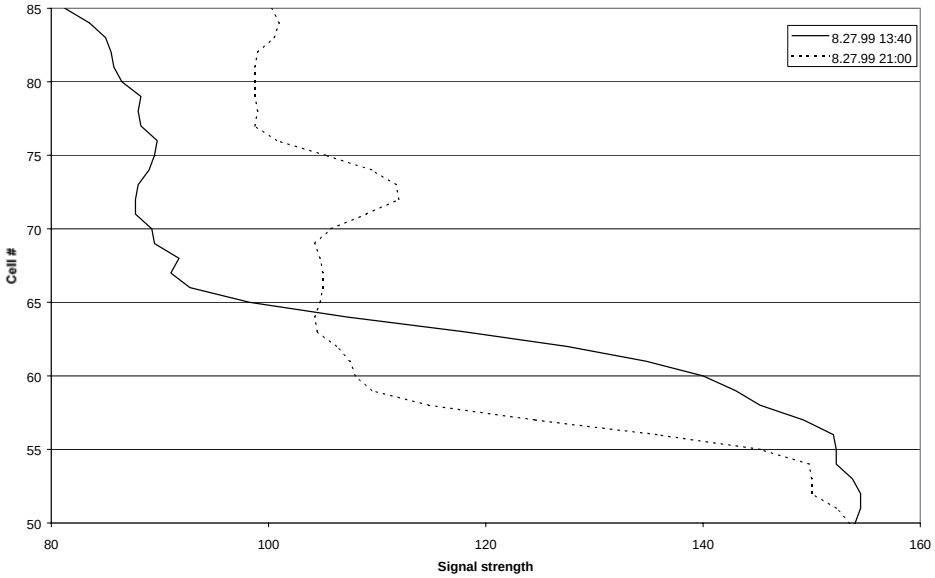

Figure 32. Signal strength from 260 – 470 m depth (Cells 85 – 50) on August 27, 1999, at daytime (solid line) and at night (dotted).

On some occasions (6-7 out of 38 days), the migration signature was not very clear. One could imagine this to be related to the local cloud cover. Thick clouds allowing less light penetration could lead the zooplankton to remain at shallower depths through (at least part of) the day. During the first few days of the ADCP measurement period, vertical velocity peaks were small or nonexistent (see **Figure 29**). At the same time, the average return signal strength was higher than the rest of the period, supporting the thought that zooplankton was present, and that a larger portion of them remained in the same depth zone. We did however not find any apparent correlation with meteorological data obtained from the Kona Airport Auhorities, the closest meteorological station to the mooring site. There were mornings with more or less overcast conditions that would or would not have vigorous downward motion in the water. It is known that cloud conditions in the area are highly influenced by island topography, and observations made on land might not be representative enough for off-shore conditions. This brief comparison of the two data sets is therefore not regarded as conclusive on the topic of zooplankton migration vs. visibility/light intensity. Another explanation to the variation in strength of the vertical velocity peaks could be that the zooplankton is found in bands, and these could be advected into and out of the observation area with the mean horizontal current. This does, however, not explain why periods with low vertical motion would also see higher signal intensity.

The vertical velocities (**Table 3**, Para. 3.1.2) showed net downward transport at all depths. This could be attributed to a downwelling area. Satellite observations of sea surface temperature during the current measurement period showed a strong negative anomaly west of the mooring site, indicating a cyclonic gyre (vortex) with cold water masses in the middle. This could in turn be compensated for by downwelling in the nearby area.

4.5 Harmonic analysis

Harmonic analyses of tidal currents were performed according to the program described by Foreman (1984) for some selected depth cells: 01, 20, 36, 53 and 78. The results for Cell 01 are presented in **Table 6**. For additional results, see Appendix B. The data were resampled to 1 hr time interval, and decomposed to N-S and E-W components. A total of 69 "deep water" harmonic constituents were included in this analysis.

The column "speed" in the resulting tables refers to the constituent frequencies used (cycles/hr) and is equal for all tables which include 36 frequencies, from zero (Z0) up to M8 (3.1 cycles/hr). Following this are the columns for the major and minor semi-axis of the current ellipses (in cm/s; positive minor axis meaning counter clockwise rotation), the inclination angle of the major axis (in degrees counterclockwise from East), the Greenwich phase angle for the constituent current vector and its rotating components (degrees, +/-).

The semidiurnal tide represents frequencies of 1/12.4 hrs ≈ 0.08/hr. This corresponds to constituents No 15-19 (N2, M2 etc). As seen from all tables (incl. the Appendix), there are significant peaks in major axis values for M2 or neighbouring constituents, reflecting the importance of the semidiurnal tide. The inclination of major axis are around 120^{o} -150^{o} (relative to east) meaning main tidal current axis is along NW-SE. This seems to correspond well with the statistics presented in Chapter 3. Also, the diurnal components (e.g. K1, luni-solar diurnal) have significant strenght at some of the investigated depths, but not all.

Table 6. Results of harmonic analysis of the current time series for ADCP Cell 1, (depth 763 m), according to the procedures by Foreman (1984). See text above for some explanation.

	COMPONENT	SPEED	MAJOR	MINOR	INC	G	G+	G-
1	Z0	.00000000	.950	.000	113.9	180.0	66.1	293.9
2	MM	.00151215	.506	.051	99.2	298.6	199.4	37.8
3	MSF	.00282193	.313	.127	115.6	150.4	34.9	266.0
4	ALP1	.03439657	.096	-.027	36.6	146.8	110.2	183.3
5	2Q1	.03570635	.156	-.050	161.2	184.1	22.9	345.2
6	Q1	.03721850	.209	.072	136.1	148.9	12.8	285.0
7	O1	.03873065	.246	-.071	98.6	31.9	293.3	130.4
8	NO1	.04026860	.535	-.113	150.7	150.2	359.6	300.9
9	K1	.04178075	.099	-.040	115.2	158.2	43.0	273.4
10	J1	.04329290	.171	-.028	52.5	28.3	335.8	80.7
11	OO1	.04483084	.733	-.080	97.0	113.4	16.3	210.4
12	UPS1	.04634299	.344	-.123	48.2	357.2	309.0	45.3
13	EPS2	.07617731	.379	-.095	88.3	115.4	27.1	203.7
14	MU2	.07768947	.258	-.111	146.9	351.0	204.1	137.9
15	N2	.07899925	.338	-.092	156.9	355.2	198.3	152.1
16	M2	.08051140	1.080	.252	126.5	242.5	116.0	9.0
17	L2	.08202355	.519	.149	135.2	196.4	61.2	331.5
18	S2	.08333334	.826	-.028	150.8	178.8	27.9	329.6
19	ETA2	.08507364	.264	.019	144.3	170.5	26.2	314.9
20	MO3	.11924210	.270	-.042	157.7	55.9	258.3	213.6
21	M3	.12076710	.333	.044	145.6	128.8	343.2	274.4
22	MK3	.12229210	.324	-.083	116.2	182.2	65.9	298.4
23	SK3	.12511410	.272	-.111	91.1	313.0	222.0	44.1
24	MN4	.15951060	.156	-.032	109.5	22.9	273.4	132.4
25	M4	.16102280	.221	.126	75.9	218.0	142.1	294.0
26	SN4	.16233260	.219	.024	174.9	65.8	251.0	240.7
27	MS4	.16384470	.375	.016	119.3	41.7	282.4	161.0
28	S4	.16666670	.301	.008	171.1	166.3	355.1	337.4
29	2MK5	.20280360	.159	-.007	169.3	192.1	22.8	1.4
30	2SK5	.20844740	.217	.059	125.3	271.3	146.0	36.6
31	2MN6	.24002200	.174	.094	104.3	179.0	74.7	283.2
32	M6	.24153420	.231	.095	86.6	70.9	344.2	157.5
33	2MS6	.24435610	.076	.002	147.6	282.2	134.6	69.8
34	2SM6	.24717810	.177	.109	94.3	59.9	325.6	154.2
35	3MK7	.28331490	.146	-.040	115.4	266.4	151.0	21.9
36	M8	.32204560	.087	-.011	113.4	314.6	201.2	68.0

4.6 Energy spectra

By running the STATISTICA™ Time Series module we created an energy spectrum of the RCM9 time series of current speed. The six most powerful peaks are summarized in **Table 7**. They are all in the very low frequency end of the spectrum (period 2.5 days or longer). Another energy maximum was found at around 0.013 cycles/10 minutes, corresponding to the 12.5 hour semidiurnal tide. Smaller local maxima corresponding to ca. 8.3 hours and ca. 6 hours were also detected.

Table 7. Energy maxima from the RCM9 time series.

Number	Frequency	Corresponding period	Spectral density
1	0.000732	9.5 days	12437
2	0.000366	19 days	11232
3	0.001099	6.3 days	11067
4	0.001831	3.8 days	9305
5	0.001953	3.55 days	9202
6	0.002686	2.58 days	8685

The spectrum shown in **Figure 33** has a low-frequency cutoff at 0.01 cycles/10 minutes (16.6 hour period) and a high frequency cutoff at the Nyquist frequency (two times the sampling interval = a 20 minute period or 0.5 cycles/10 min). By excluding the low-end part (including the diurnal tide), some higher frequency peaks are appearing e.g. at 0.15 (1.1 hour period), 0.27 (37 min period), 0.43 (23 min period) and 0.47 (21 min period). The semidiurnal tide had a significant peak at 0.013, which is just at the low end border.

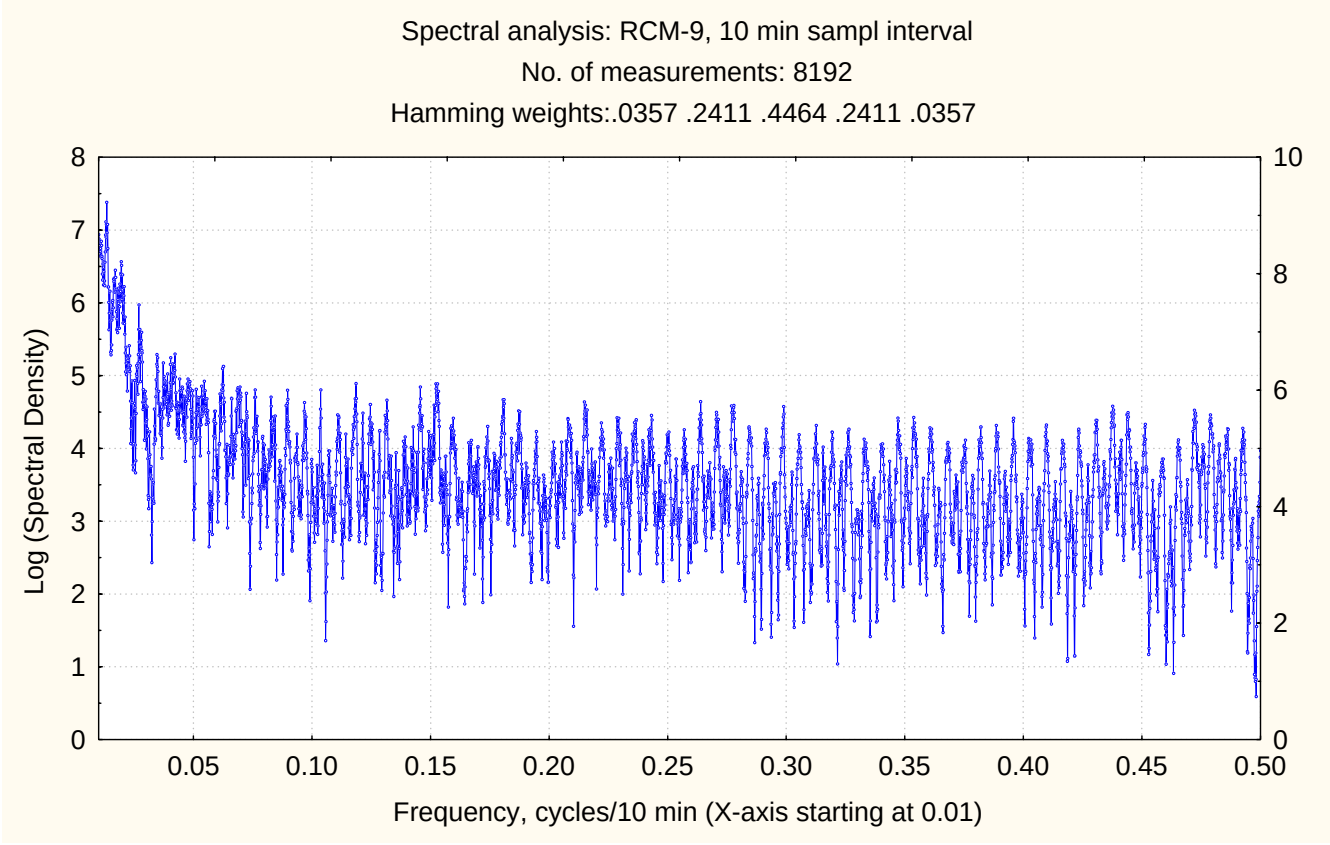

Figure 33. Energy density spectrum ($cm^2/s^2/\Delta f$) of the measured current velocity 8 m above the bottom with the Aanderaa RCM-9 Doppler current meter. The sampling period was 10 minutes. Only the higher-frequency part (period < 16.6 hours) of the spectrum is shown.

In terms of the higher frequencies, it may be relevant to refer to some internal wave theory and to CTD obervations made in August 1999, prior to deployment of the moorings (Sundfjord et al. 1999) and to previous mesurements. The observed local buoyancy frequency N in August, 1999, decreased from values above 0.01 rad/s (10 min period) in the upper layer to minimum values of 0.002-0.004 rad/s (50-25 min period) closer to the bottom. Nihous and Vega (1997) reported average N-values from older data at the level of the seawater intake at 670 m depth off Keahole Point of 0.0036 rad/s (5.7 x 10^{-4} Hz or 29 minute period) which is comparable to the values derived from the 1999 CTD material. At any rate, the N-values represent the high cutoff frequency for internal gravity waves and observed oscillations of this kind will probably have lower frequencies. When again refering to the energy spectrum from the RCM-9 data there are some peaks both above and below the cited N-values. Those with longer periods, e.g. above 1 hour, can reflect internal gravity waves.

Sloping seafloor topography can reduce the oscillating frequency ω for internal waves (Cushman-Roisin 1994), according to the formula: $\omega = N \tan\beta/\{1 + \tan^2\beta\}^{1/2}$ (rad/sec), where β represents the seafloor slope angle and the effect of earth rotation and some other factors have been neglected for simplicity. With $\beta = 25°$ and N = 0.0036 rad/s, internal wave amplification could occur at $\omega = 1.5 \times 10^{-3}$ rad/s (70 min period) (Nihous and Vega 1997). Similarly, resonant period values can be calculated from the 1999 deep CTD data at about 2.1 hours. We actually see a period of 1.1 hour in the RCM-9 spectrum, corresponding to Nihous and Vega's calculations. A 2.1 hour period would correspond to a peak at 0.08 in the RCM-9 spectrum, while a close peak is seen at 0.065. Such a modest frequency shift may be induced by the current.

4.7 Event duration analysis

4.7.1 Method

We have analysed some of the ADCP depth cell time series for the distribution of periods where

1: the current speed was continuously below or above selected threshold values, and
2: the current direction was continuously within (or outside of) a specified sector.

This kind of "duration analysis" toolware has been used by meteorologists when describing wave climate. NIVA applied similar computations when describing circulation at fish farm sites (Nygaard and Golmen 1997) and near plume outfalls. The method focuses on the duration of events, I.e. for how long time a certain current condition is satisfied prevailingly and uninterruptedly. It is distinct from the common cummulative statistics made on current data. For fish farms it is important to know how long periods with weak currents can be expected, so that the biomass and density can be controlled accordingly. For an outfall plume knowing for how long periods the current remains steady in one direction is important information when assessing the theoretical impact zone.

As the CO_2 experiment will involve release of CO_2 that will rise and probably form some kind of plume, we thus thought that similar analysis and information might be useful for the planning of the CO_2 experiment, both for initial theoretical modelling, for timing of actual releases and for the subsequent monitoring. The box below describes to some detail, the method.

Event Duration. Brief method description.

Assume a time series X(t) describing a physical phenomena, e.g. measured current speed, with n equally spaced samples totally,

$$X(t)=x_1, x_2, x_3,...x_n = x(t_1), x(t_2), x(t_3),...x(t_n)$$

We assume that the (time limited) time series does map to a satisfactory degree the variability of the real process or parameter we are studying (e.g. current speed or direction). This implies that the interval between measurements is sufficiently short to detect interesting short term variability, and that the total length of the time series also is sufficient to reveal long-term variability. If the variability is "stationary" some more formalism can also be derived.

The total length of the time series is τ with a constant sampling interval Δ:

$$\tau = (n-1)*\Delta.$$

By traditional spectral analysis one assumes stationarity of the periodicity over a range of frequencies between $1/2\tau$ and $1/2\Delta$. The "duration analysis" does not have such restrictions. Similarly, cumulative statistics do not take into account the relationship among neighbouring observations. The present method determines the number of periods e.g. when the current constantly remains below or above a selected value V_j. Depending on the selected value of V_j, this may give many or few periods, and with different durations.

The total number of such periods is an important information, but not sufficient for many purposes. It is also important to know the length (duration) of these periods, and the individual distribution thereof. The shortest periods possibly resolved will be of length Δ. The next ones $2*\Delta$, etc.

For a given V_j we get a "duration vector" $T_j(k)$ with k elements consisting of N_k periods of given duration:

$T(N_k) = (N_1*\Delta, N_2*2\Delta, N_3*3\Delta, N_4*4\Delta.....N_k*k\Delta)$.

k = selected integral number, $\leq$ n-1, giving k maximum equal to $(n-1)=\tau/\Delta$. I.e. $k_{max}*\Delta = \tau$.

By successively scanning the time series X by varying V_j, j=1,2,3,..m, (e.g. 2 cm/s, 3 cm/s, 4 cm/s, 5 cm/s, 6 cm/s...), we get the result as a duration matrix N with elements consisting of counted numbers of periods. The matrix has m columns and k rows. The column values will represent numbers of periods with corresponding to certain current speeds V_j, and the rows (lines) the number of periods with certain length (duration) T_k. A similar method can be applied to current direction data, temperature series etc.

4.7.2 Results for current speed

Analyses have been performed on the RCM-9 data near the bottom, for the deepest and shallowest ADCP cell, and for every 50 m depth in between. An example is shown in **Table 8**, for ADCP Cell No. 11 (700 m depth). **Figure 34** corespondingly shows a graphical presentation for three different parameters that may be particularly relevant for the CO_2 experiment. Similar results are presented in Appendix C.

For Cell No. 11, the results show that the average duration of periods currents stay below 1 cm/s is 44 minutes (0.74 hours). The longest period below 1 cm/s was (only) 2 hours. The longest period that currents stayed above 1 cm/s was 51.3 hours, and the corresponding average period was 10.5 hours. For stronger currents, e.g. 10 cm/s, the current on the average stayed below this value for 22.5 hours, and the longest period it stayed below 10 cm/s was 122 hours. Similar types of statistics can be derived for other test values and parameters.

Table 8. Results from duration analysis of current speed for data from ADCP Cell 11, 700 m depth.

```
Cell number 11.
Mean current   4.61   Fmax =      17.40 Variance=       7.32
Tot# of measurements=  1355 Equal to  903.3 hrs or   37.6 days
Finding duration of periods with speed less than/= celected Speed(V):
Speed:      Less or equal to (V)
#:          Number of single samples l/eq. Speed
%:          % distribution of # (simple cumulative distr.)
Periods:    Number of periods with samples with current l/eq. Speed, V
mpu:        Mean period length (min) (hrs), current l.eq. Speed, V
lpu:        Longest period (hrs) w/ current l.eq. Speed, V
mpo:        Mean length of periods(min)(hrs) w/current g.eq. Speed, V
lpo:        Longest period w/current g.eq. Speed, V.
```

Speed	#	(%)	#periods	mpu		lpu	mpo		lpo
				minutes	hrs	hrs	minutes	hrs	hrs
1.00	89	6.57	80	44	0.74	2.0	633	10.55	51.33
1.50	137	10.11	117	47	0.78	2.0	416	6.94	35.33
2.00	214	15.79	151	57	0.94	2.7	302	5.04	28.67
4.00	637	47.01	224	114	1.90	8.7	128	2.14	16.00
6.00	988	72.92	152	260	4.33	27.3	97	1.61	6.67
8.00	1190	87.82	80	595	9.92	47.3	82	1.38	4.67
10.00	1287	94.98	38	1355	22.58	122.0	72	1.19	3.33
15.00	1351	99.70	3	18013	300.22	405.3	53	0.89	2.00
20.00	1355	100.00	1	54200	903.33	903.3	0	0.00	0.00
25.00	1355	100.00	1	54200	903.33	903.3	0	0.00	0.00

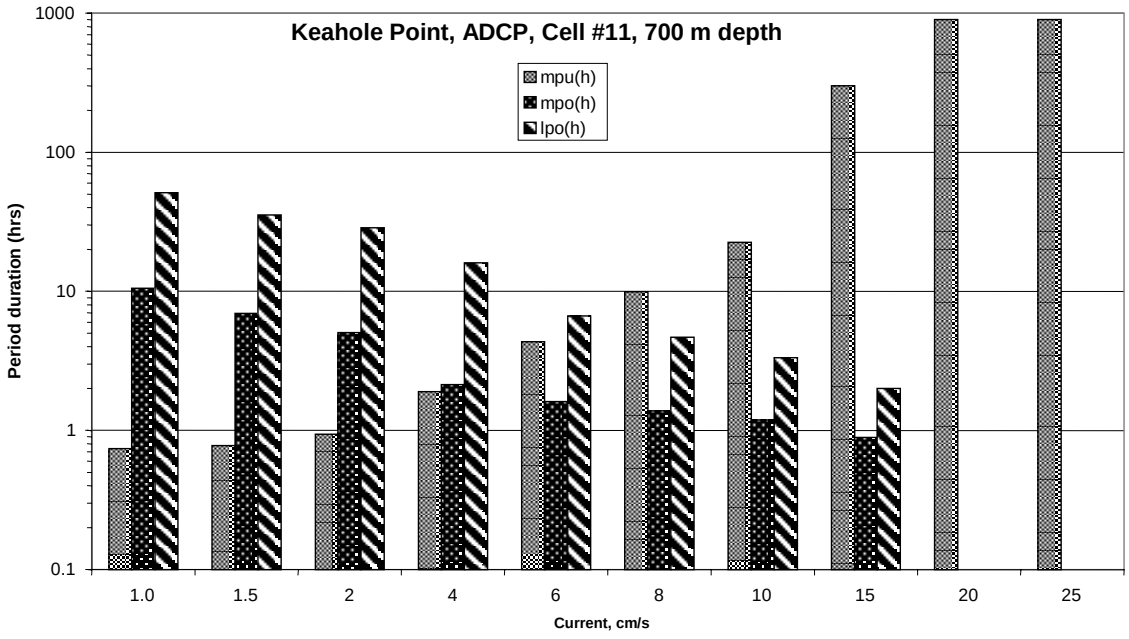

Figure 34. Some results of the duration analyses for current speed, Cell 11 (700 m). Values in hours. Mpu: Mean length of periods with currents continuously under selected current speed values (X-axis). Mpo: Mean length of periods with current above selected values. Lpo: Longest period with currents exceeding selected current.

4.7.3 Results for current direction

Results for current direction, Cell 11, are shown in **Table 9** with some selected values plotted in **Figure 35**. Similar results for other cells, corresponding to those selected for current speed, are presented in Appendix C.

Results for Cell 11 are relatively evenly distributed. There are no sectors with a significantly higher representation. Most single samples and periods are found in sectors of SE direction. This is as expected from the current roses show previously. Mean period duration within sectors are around 1 hour for every sector, with no characteristic peak. Also, the longest periods with current staying inside the selected sector are found on the SE-ward side. The current naturally fluctuates even if it has some evident "mean" direction. Selecting rather narrow sector bins (30^o in our calculations) will naturally result in "noise" and rather low period values. Widening the sector will render longer periods.

Table 9. Results for duration analysis, current direction, Cell 11, 700 m depth.

```
Direction:  Center value of 30 degree directional sector
#:          Total number of samples inside sector
%:          Percentage of samples inside sector, relative to whole series
Periods:    Number of periods @£@ is distributed over
mpi:        Mean period (minutes,hours) of periods inside sector
lpi:        Longest period inside sector
mpo:        Mean period outside sector
lpo:        Longest period outside sector
```

Direction	Samples		periods	mpi		lpi	mpo		lpo
(o)	#	%	#	minutes	hours	hrs	minutes	hrs	hours
15	63	4.65	57	44	0.74	1.3	907	15.11	64.67
45	51	3.76	49	42	0.69	1.3	1064	17.74	68.67
75	50	3.69	47	43	0.71	1.3	1111	18.51	90.67
105	152	11.22	129	47	0.79	2.7	373	6.22	55.33
135	345	25.46	197	70	1.17	5.3	205	3.42	25.33
165	237	17.49	174	54	0.91	4.7	257	4.28	26.67
195	98	7.23	89	44	0.73	2.0	565	9.42	42.67
225	56	4.13	49	46	0.76	2.0	1060	17.67	96.00
255	38	2.80	37	41	0.68	1.3	1424	23.73	139.33
285	68	5.02	62	44	0.73	1.3	830	13.84	66.00
315	95	7.01	68	56	0.93	3.3	741	12.35	83.33
345	102	7.53	76	54	0.89	2.0	659	10.99	72.67

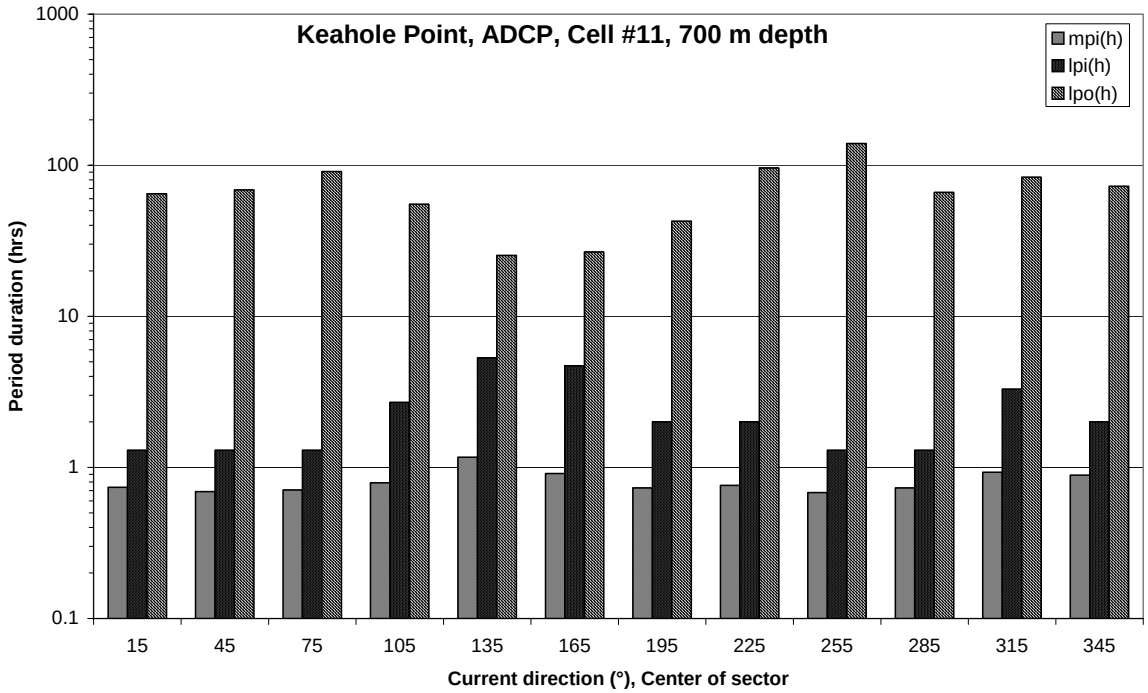

Figure 35. Results for duration analysis, current direction, for ADCP Cell 11, (700 m depth). Values are in hours. Mpi: Mean duration for periods with current inside sector. Lpi: Longest period inside sector. Lpo: Longest period outside sector.

4.8 Comparison between moorings and instruments

The mooring supplied by RITE/CRIEPI in Japan with three current meters was deployed ca. 1/2 n. mile north of the ADCP mooring (**Figure 2**). Results have been reported by Maeda et al. (2000), however with no comparisons made with the data from the ADCP mooring. Therefore we attempt to make a brief descriptive comparison between the results here. The instruments used in the Japanese mooring were 3D-ACM self-recording acoustic current meters from Falmouth Scientific Inc. The sampling interval was 2 minutes, i.e. more rapid than the ADCP and the RCM9. The depths of the instruments are shown highlighted in **Table 10**.

The Japanese mooring was located at 874 m bottom depth and ca 1.2 mile offshore, while the ADCP mooring was at 790 m depth, slightly closer to shore. In principle both the horizontal separation of the moorings and the different distance from shore may explain differences in measurement results. In addition, different measurement principles, sampling intervals and mooring systems can lead to somewhat different results.

For the two upper ACM instruments the comparison with the corresponding ADCP depth cells for mean speed is excellent. The ACMs sampled slightly higher max. values, but this is probably due to their more rapid sampling of every 2 minutes compared with the ADCP's 40 minute averages. The differences in dominating current direction (mean vector direction) was 10^o -20^o, which also may be regarded as very satisfactory, also taking into consideration the fact that the ADCP compass was not re-calibrated when mounted in its steel frame.

The deepest ACM was about 80 m deeper than ADCP Cell 01 and 63 m deeper than the RCM9, so a direct comparison between this ACM and the other mooring may be misleading. The mean speed for ADCP Cell 01 was 4.39 cm/s, and maximum speed was 24.2 cm/s. The RCM9 was about 17 m deeper

than Cell 01 and thus a bit closer to the deepest ACM. Average speed for the RCM9 was 4.25 cm/s, and maximum speed was 14.7 cm/s (**Table 10**).

The constant decrease of mean speed with depth, all three instrument types considered, is striking and in accordance with the general conception of open ocean circulation. Also maximum speed follows roughly the same pattern, with the exception of ADCP Cell 01, which had an extra high maximum value. According to **Figure 7**, this cell had several occasions with currents exceeding 15 cm/s. The previous Event Duration Analysis showed that these events lasted only very short time.

Effects of the drag on the Japanese line mooring were already discussed by Maeda et al. (2000). Lateral displacement during shift in current direction og strong bursts may have caused a negative bias in the maximum current values of the ACMs. Despite these and other possible disturbing factors, the over-all comparison of results between moorings and instruments shows a high degree of correspondence and similarity.

Table 10. Comparison between the Japanese and the ADCP mooring results, where applicable. Only horizontal speed is considered. No direct comparison can be made with the deepest Japanese ACM instrument. The deepest cell of the ADCP was at 763 m, and the RCM9 below was at 780 m depth.

	Japanese mooring				**ADCP mooring**		
Instr. depth (m)	Mean speed (cm/s)	Max speed (cm/s)	Main direction (^{o})	Nearest cell #	Mean speed (cm/s)	Max speed (cm/s)	Main direction (^{o})
407	7.03	25.1	332	60	7.28	23.1	322
631	4.98	19.6	163	23	4.97	17.7	143
763	-	-	-	01	4.39	24.2	157
780	-	-	-	RCM 9	4.25	14.7	117
790	-	-	-	Bottom depth, ADCP mooring			
854	4.17	15.2	139				
874	Bottom depth, Japanese mooring						

4.9 Concluding remarks

The final ADCP data consist of a time-depth matrix each for horizontal current velocity, direction, vertical current velocity and signal strength. Each matrix has 85 rows (depth cells 01 – 85) and 1354 columns (simultaneous profiles or "ensembles" for each 40 minutes). We have analysed the rather voluminous data to some extent, leaving room for more in-depth analyses for those interested and as specific demand emerges.

The measurements serve several purposes:

1. Describe the ambient current field at the location of the proposed CO_2 discharge in terms of:
    - Mean current speed and prevailing direction at many different depths
    - Vertical distribution of currents at many instants, from ca 250 m depth to 780 m depth.
    - Maximum and minimum currents
    - Vertical shear
    - Time variability of current and duration of specific situations

2. Provide input numbers for ambient current and near-bottom current as required for the dynamic numerical models (plume and near-field).

- Ambient current
- Near-bottom current
- Vertical shear
- Variability in time of current and shear
- Vertical velocity and "slip velocity"
- Energy at low-frequency end of turbulence spectrum

3. Provide input data for the planning and design of ROV operations (umbilical strain etc.)

4. Provide input data for pipeline deployment and handling.

It is anticipated that the data also can have some general interest in connection with oceanographic investigations around Hawaii. The upcoming HOME (Hawaii Ocean Mixing Experiment) is one such programme, that includes a field survey and measurement campaign starting in year 2000 (D. Luther, U of Hawaii, pers. comm.). Mid-ocean ridges are expected to play an important role in the turbulent mixing in the mid and low latitude ocean. A major goal of the across-ridge surveys is to locate sites of intense tidal mixing. Similar sites located elsewhere on the continental slopes may in the future become important sites for permanent CO_2 injection if this technology is implemented on a large scale. Thus it is important for the CO_2 ocean sequestration community to communicate with other oceanographic research groups, and exchange data.

The planned CO_2 release experiment is made to help scientists, modellers and engineers to improve their understanding of how liquid CO_2 behaves when injected in the deep ocean. Direct observations and measurements of the plume and droplets should be made by simultaneously acquiring information about the ambient background field of hydrography, ocean chemistry, marine biology, local sediments and currents. Without such information, monitoring and sampling may become difficult, and the interpretation of observations may become uncertain and dubious.

The planned CO_2 release will last for 1-2 weeks totally, with shorter time interruptions in between. The CO_2 droplets are expected to rise in the water column, maybe 100 m or more. As the CO_2 gradually dissolves into the seawater, denser water is formed which is expected to sink before interleaving in the water column, or form a dense plume along the bottom. In order to optimize the monitoring of the CO_2 plume during the experiment and to interpret the results, it is important to have some information in real time or near real-time of the currents at the depth range of the plume. It has thus been suggested to have the ADCP connected to an acoustic modem for transfering real-time data to the surface, to serve this purpose. An alternative is to transfer data via a cable to shore, to a surface buoy or to a vessel. The ADCP might also be suspended in a signal cable from a vessel, looking downwards towards the bottom. The 40 minute sampling interval which was used in 1999 should be made shorter (< 10 minutes) in order to get more rapid updates and more information on background turbulence.

The ADCP dataset obtained and partially presented here, can be studied further in order to optimize the release experiment and the monitoring. Crucial for this planning is information on how steady the current is, and under what conditions or tidal phases it tends to become more variable. Running the experiment under a weak and steady current situation is preferable from a sampling and monitoring viewpoint. But the results in the present report show that the currents never stay steady for a long time. Either it changes speed, or it changes in direction. The Duration and Event analyses as described in the report give some information about this. The analyses may be further refined through a dialogue between the modelers and the oceanographers.

5. References

Cushman-Roisin, B. 1994: Introduction to Geophysical Fluid Dynamics. Prentice Hall, New Jersey, 320 p.

Flament, P., S. Kennan, R. Lumpkin, M. Sawyer, E.D. Stroup, K. Bigelow, P. Caldwell, J. Firing, B. Kilonsky, C. Motell, J. Potemra, F.Santiago-Mandujano and M. Seki 1996: The Ocean Atlas of Hawaii. Rep. SOEST, University of Hawaii, (web-pages).

Foreman, M.G.G. 1984: Manual for Tidal Currents. Analysis and Prediction. Rep. IOS, Sidney, Canada, 70 pp., 3rd reprinting.

Gordon, R. L. 1996: Acoustic Doppler Current Profiler - Principles of operation: a practical primer. RD Instruments, San Diego, California, 54 p.

Maeda, Y., Y. Koike, K. Shitashima, N. Nakashiki and T. Ohsumi 2000: Direct measurements of Currents in West Coast of Hawaii Island (1.2 miles offshore of Keahole Pt.). Technical note, CRIEPI, Japan, 15 p.

Mylvaganam, S and T. Jakobsen (1999): Turbidity sensor for underwater applications. Technical note, Aanderaa Instruments, Bergen, 4 p.

Nihous, G. and L.A. Vega 1997: Internal waves on a Deep Sloping Seafloor off the West Coast of Hawaii. Technical Note, Dept. of Engineering, U of Hawaii, 10 p.

Nygaard, E. and L.G. Golmen 1997: Current conditions at fish farm sites in relation to topography and environmental conditions. Rep. No. 3709, NIVA Bergen/Oslo, 58 p (in Norwegian).

Parsons, T. R. and M. Takahashi 1977: Biological Oceanographic Processes, Pergamon Press, 332 pages.

Sundfjord, A., L. G. Golmen and Y. Maeda 1999: CTD data report from R/V "KOK" cruise 05-99 3-8 August, 1999. Report no. SNO 4104-99, NIVA, 59 p.

Rippeth, T. P. and J. H. Simpson 1998: Diurnal signals in vertical motions on the Hebridean Shelf. Limnology and oceanography, 43(7), 1690-96.